Journal of Molecular Graphics and Modelling 50 (2014) 16–34

Contents lists available at ScienceDirect

Journal of Molecular Graphics and Modelling

journal homepage: www.elsevier.com/locate/JMGM

Designing of multi-targeted molecules using combination of molecular screening and *in silico* drug cardiotoxicity prediction approaches

Birce Buturak[a], Serdar Durdagi[b], Sergei Y. Noskov[c,*], A. Tugba Ozal Ildeniz[a,d,**]

[a] Computational Biology and Bioinformatics, Graduate School of Science and Engineering, Kadir Has University, Istanbul, Turkey
[b] Department of Biophysics, School of Medicine, Bahcesehir University, Istanbul, Turkey
[c] Institute for Biocomplexity and Informatics, University of Calgary, Calgary, AB, Canada
[d] Department of Bioinformatics and Genetics, Kadir Has University, Istanbul, Turkey

ARTICLE INFO

Article history:
Accepted 11 February 2014
Available online 6 March 2014

Keywords:
Protein database search
Molecular docking
Molecular engineering
Carbonic anhydrase inhibitors
Multi-targeted agents
hERG ion channel

ABSTRACT

We have previously investigated and reported a set of phenol- and indole-based derivatives at the binding pockets of carbonic anhydrase isoenzymes using *in silico* and *in vitro* analyses. In this study, we extended our analysis to explore multi-targeted molecules from this set of compounds. Thus, 26 ligands are screened at the binding sites of 229 proteins from 5 main enzyme family classes using molecular docking algorithms. Derived docking scores are compared with reported results of ligands at carbonic anhydrase I and II isoenzymes. Results showed potency of multi-targeted drugs of a few compounds from investigated ligand set. These promising ligands are then tested *in silico* for their cardiotoxicity risks. Results of this work can be used to improve the desired effects of these compounds by molecular engineering studies. In addition these results may lead to further investigation of studied molecules by medicinal chemists to explore different therapeutic aims.

1. Introduction

The rational drug design strategy for screening single-targeted and highly specific ligands was widely investigated in last decade [1,2]. In spite of appealing simplicity of the approach, there are large number of complex diseases (*i.e.*, cancer, cardiovascular diseases, neurodegenerative diseases, rheumatoid arthritis) where single-target strategy fails. For example, many high affinity agonists or antagonists of specific receptors are known for altering cell function by simultaneous binding to number of other targets. Systems biology and network control analysis have shown that complex diseases are solid against perturbations and are always controlled by more than one biochemical pathways and processes in cells [2]. Although poly-pharmacology is naturally associated with drug toxicity and off-target side effects, especially when rationally designed, they can have larger therapeutic window [1,2]. For example, patients with mild cognitive disorders and risk of Alzheimer's disease dementia are often considered for the treatment using anti-hypertensive drugs. Angiotensin II (Ang II) type 1 (AT1) blockers are used for patients with intolerance for ACE inhibitors or if these inhibitors do not provide the desired effects [3–5].

We have previously investigated a set of phenol- and indole-based derivatives for their effect to inhibit carbonic anhydrase (CA) targets with *in silico* and *in vitro* approaches [6,7]. These compounds showed sub-micromolar to low micromolar affinity to the CA isoenzymes. In this study, our main goal was to investigate multi-target interactions and multi-functional potentials of these compounds. For this aim, molecular docking of 26 ligands into binding sites of 229 proteins from different classes were performed to determine potential interactions of these ligands with the active site residues.

The 2D structures for ligands considered in this study are collected in Table 1. The target enzymes used in this study are classified according to the reactions they catalyze (see Section 2 for selection of target enzymes). The five classes that screened in this study are: transferases (Class-II), hydrolases (Class-III), lyases (Class-IV), isomerases (Class-V), and ligases (Class-VI) [8–10]. Transferases (Class-II) catalyze transfer (*i.e.*, movement) of a functional group from one molecule to the other. A broad variety of functional groups are targeted by the corresponding transferases, which include phosphate, glycosyl and methyl groups. The corresponding

* Corresponding author.
** Corresponding author at: Computational Biology and Bioinformatics, Graduate School of Science and Engineering, Kadir Has University, Istanbul, Turkey.
E-mail addresses: snoskov@ucalgary.ca (S.Y. Noskov), tugba.ozal@khas.edu.tr (A.T.O. Ildeniz).

http://dx.doi.org/10.1016/j.jmgm.2014.02.007
1093-3263/

Table 1
Molecular structures of the tested (docked) compounds [6,7].

Comp. no.	2D structures	Comp. no.	2D structures
1	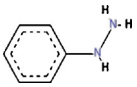	2	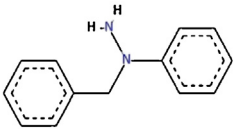
3	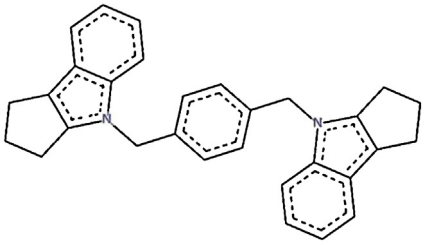	4	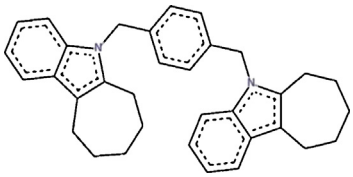
5	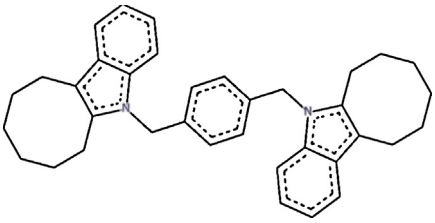	6	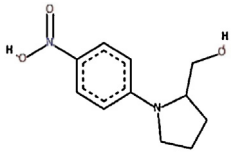
7	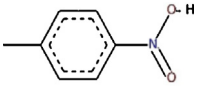	8	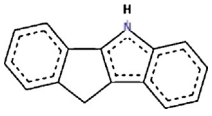
9	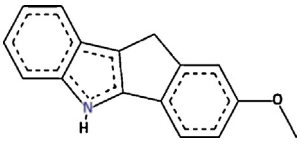	10	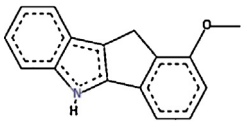
11	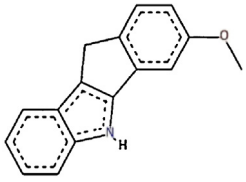	12	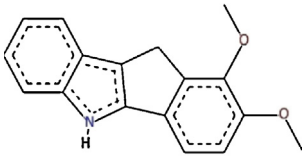
13	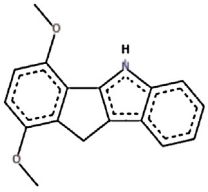	14	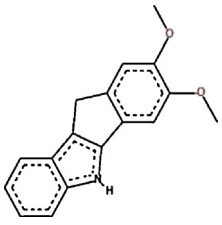
15	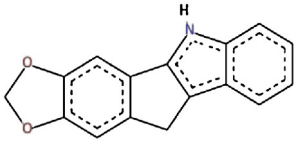	16	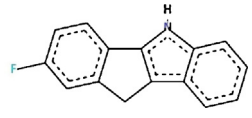
17	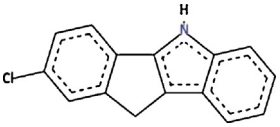	18	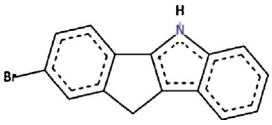

Table 1 (*Continued*)

Comp. no.	2D structures	Comp. no.	2D structures
19	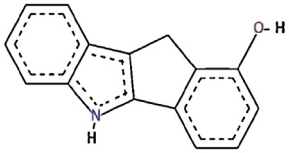	**20**	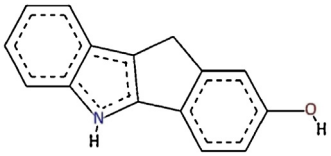
21	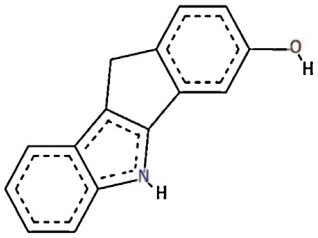	**22**	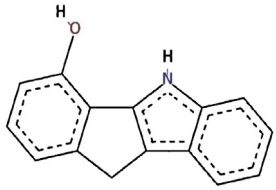
23	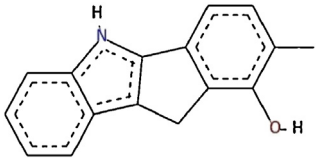	**24**	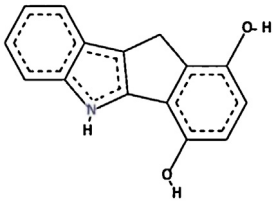
25	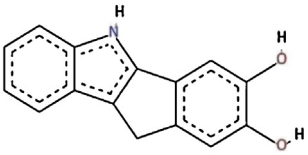	**26**	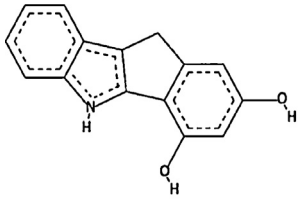

reaction is: AX + B → A + BX; where A is the donor, B is the acceptor and X is functional group. Transferases have two sub-groups kinases and deaminases. Kinases participate in catalyzing the transfer of phosphate groups during phosphorylation. Therefore, they are effective on different molecules, for example nucleotides, lipids and carbohydrates. The most important clinically group of kinases comprises enzymes participating in a signal transduction and therefore in a control of complex processes within the cell. Kinases are classified into more than 500 different types in human. The deaminases form another group of transferases. They catalyze the transfer of amino groups. Hydrolases (Class-III) catalyze hydrolysis reactions. They allocate substrates with addition of water molecule at the point of cleavage. The corresponding reactions is: $A–B + H_2O \rightarrow A–OH + B–H$. Hydrolases are sub-divided into several subclasses, such as lipases cleaving ester bonds in fatty acids and glycerol, nucleases involved in hydrolysis of nucleic acids, proteases for proteins, *etc.* Lyases (Class-IV) which catalyze lysis reactions are type of elimination reaction, that are not hydrolytic or oxidative. These reactions catalyze an addition reaction, where a substrate is added to a double bond. These reactions are usually applied to as synthase enzymes. A lyase reaction would be, ATP ↔ cAMP + PPi. Lyases involve oxalate decarboxylase and isocitrate lyase. Isomerase enzymes (Class-V) catalyze structural changes within a molecule. An isomerase reaction would be, A → B, where B is an isomer of A. Isomerases involved in many biochemical pathways, for example; the citric acid and the glycolitic pathway. They include triose phosphate isomerize, photoisomerase and bisphosphoglycerate mutase. Isomerases can help in the conversion of citrate to isocitrate in the citric acid cycle. They can catalyze phosphorylation reaction pathway throughout the Krebs Cycle by preparing the molecule for oxidation states. Finally, ligases (Class-VI) catalyze ligation. Since this catalysis requires chemical potential energy, the reaction is incorporated with the hydrolysis of a diphosphate bond in a nucleotide triphosphate such as ATP. The most important hydrolases enzyme is the DNA ligase enzyme which catalyses the ligation between breaks in DNA by forming a phosphodiester bond. These enzymes are further sub-divided into several types. Each type is involved with catalysis of repair reactions for different bond types. For example DNA ligase-I repairs single stranded breaks using the complementary strand as a template, like in DNA replication of the lagging strand.

Thus, in this study, 26 ligands are screened using molecular docking approach at the 229 enzyme targets from 5 different classes. Promising ligands with multi-targeted pharmacology potential are further tested for their cardiotoxicity risks by assessing their binding to the hERG1 potassium channel [11,12].

2. Methods

All docking computations performed in this study were carried out on a workstation of multithread 12 core Linux (x86-64bit) computer. Parallel processing within the multithreading were used during the docking simulations. The software used in this study was Autodock Tools [13]. Furthermore, the 2D and 3D molecular drawings, all figures of molecular structures were created with Discovery Studio 3.5(DS) [14].

Table 2
Molecular docking results (docking scores in kcal/mol) of compounds in Table 1 at the transferases (Class-II) (3 compounds could not derive a successful docking pose thus their docking scores are not tabulated). A color map is used for better visualization using certain threshold values of docking scores, such as derived docking scores values smaller than −9 kcal/mol were indicated with red color, values between −7 and −8 kcal/mol were colored with orange, values between −5 and −6 kcal/mol were given in yellow color and finally values greater than −5 kcal/mol were colored with gray.

	L1	L2	L3	L4	L7	L8	L9	L10	L11	L12	L13	L14	L15	L16	L17	L18	L19	L20	L21	L22	L23	L25	L26
1B4F	-4.12	-5.9	-7.12	-8.7	-4.95	-5.26	-6.02	-6.05	-6.4	-6.09	-5.75	-5.7	-5.92	-5.37	-5.87	-5.74	-5.52	-5.4	-5.69	-5.28	-6.13	-6.37	-5.39
1BLX	-4.36	-5.52	-8.24	-9.8	-5.15	-5.12	-5.97	-6.84	-6.02	-6.47	-6.62	-6.65	-6.78	-5.59	-5.97	-6	-5.75	-6.02	-5.55	-5.85	-6.29	-6.06	-5.45
1BTK	-4.08	-5.54	-7.01	-8.18	-4.42	-6.18	-5.71	-5.94	-5.86	-5.75	-6.2	-5.86	-6.98	-5.34	-5.49	-5.67	-5.26	-5.8	-6.03	-6.09	-5.83	-6.2	-6.09
1BX4	-4.25	-5.8	-8.38	-9.47	-4.9	-5.78	-5.92	-6.22	-6.02	-6.31	-6.64	-6.22	-6.63	-5.88	-6.32	-6.38	-6.04	-5.99	-6.02	-6.06	-6.42	-6.93	6.3
1BZY	-4.29	-5.99	-7.18	-7.78	-5.41	-5.25	-6.22	-7.14	-5.98	-5.39	-5.62	-6.47	-6.22	-6.19	-6.82	-6.97	-6.33	-6.18	-6.62	-6.29	-7.05	-7.07	-6.82
1CB0	-4.27	-5.08	-7.89	-8.7	-4.5	-6.17	-6.19	-7.19	-6.11	-6.28	-5.93	-5.87	-7.62	-6.34	-6.38	-6.57	-6.64	-6.38	-6	-6.43	-6.57	-6.16	-12.5
1CZA	-4.13	-5.78	-8.61	-9.08	-4.71	-5.7	-6.15	-6.54	-6.68	-6.64	-6.5	-6.92	-6.83	-6.47	-6.47	-6.63	-7.35	-6.38	-4.88	-4.7	-5.08	-5.03	-4.07
1E8Y	-4.38	-6.67	-8.48	-9.83	-5.45	-6.26	-7.79	-6.77	-6.81	-6.75	-7.84	-6.67	-6.5	-6.16	-6.56	-6.69	-7.21	-6.07	-5.37	-5.05	-5.65	-6.04	-8.06
1EH6	-4.58	-5.98	-7.75	-9.85	-5.29	-6.82	-6.33	-6.21	-6.24	-6.73	-6.28	-6.83	-7.58	-6.02	-6.19	-6.22	-6.43	-6.13	-6.01	-6.64	-6.53	-6.71	-6.74
1EX0	-4.73	-6.14	-9.65	-11.2	-4.74	-4.72	-7.07	-8.01	-7.47	-7.13	-7.37	-8.29	-6.53	-7.08	-7.57	-7.5	-6.49	-7.25	-5.05	-5.95	-5.95	-6.15	-5.34
1FGK	-4.29	-6.4	-9.04	-10.4	-5.46	-5.42	-6.57	-6.66	-6.43	-6.84	-6.77	-6.51	-7.17	-6.08	-6.28	-6.41	-6.11	-6.26	-5.47	-5.42	-5.47	-5.62	-5.16
1FMK	-4.2	-5.97	-8.32	-9.69	-4.58	-5.68	-6.95	-7.05	-6.9	-6.95	-7.55	-7.14	-6.65	-6.45	-6.92	-7.04	-6.27	-6.41	-6.32	-6.71	-6.67	-6.81	-5.88
1FW1	-3.89	-5.44	-7.3	-8.92	-5.11	-6.24	-5.92	-5.85	-5.98	-5.74	-6.25	-5.77	-6.97	-5.22	-5.49	-5.61	-5.3	-5.61	-5.44	-5.68	-6.14	-6.17	-5.21
1G3M	-4.54	-6.06	-6.69	-7.68	-5.06	-7.56	-8.02	-8.31	-8.24	-8.1	-8.23	-8.59	-9.69	-7.47	-7.97	-8.13	-7.57	-7.19	-7.39	-7.12	-7.72	-7.9	-6.88
1G55	-4.13	-5.78	-9.1	-9.68	-4.51	-5.18	-6.1	-6.52	-6.38	-6.39	-6.44	-6.47	-6.64	-6.11	-6.43	-6.47	-6.44	-6.24	-6.43	-5.85	-6.63	-5.4	-5.9
1GZ8	-4.67	-5.55	-8.31	-9.25	-5.08	-6.09	-6.43	-6.53	-6.72	-6.12	-6.78	-6.41	-7.11	-6.26	-6.54	-6.61	-6.48	-6.67	-5.57	-6.34	-6.33	-6.6	-6.06
1HE7	-4.01	-5.92	-7.27	-8.8	-4.59	-5.62	-6.02	-6.5	-6.79	-6.28	-6.49	-6.99	-6.54	-6.2	-6.53	-6.68	-6.09	-6.24	-6.82	-5.74	-6.84	-6.8	-5.8
1HML	-3.85	-5.14	-7.4	-8.38	-3.93	-4.34	-5.69	-5.68	-5.24	-5.78	-5.54	-5.39	-5.08	-5.46	-5.34	-5.29	-5.79	-5.96	-6.2	-5.07	-6.42	-6.46	-5.09
1I1N	-4.6	-6.07	-7.34	-8.64	-4.66	-5.49	-7.88	-6.82	-6.7	-6.86	-6.78	-7.2	-5.95	-6.29	-6.66	-6.66	-7.21	-6.5	-6.76	-6.12	-6.88	-6.73	-6.03
1J1B	-4.72	-6.19	-8.72	-9.33	-5.18	-6.8	-6.57	-7.15	-6.75	-7.53	-6.25	-7.09	-8.43	-6.16	-6.56	-6.71	-6.16	-6.16	-6.71	-7.62	-6.61	-6.42	-6.19
1J99	-3.9	-6.13	-8.74	-10.1	-4.91	-6.24	-6.89	-6.93	-7.28	-7.08	-6.57	-7.2	-7.42	-6.53	-6.85	-7.01	-6.13	-6.07	-6.22	-6.16	-10.6	-7.01	-5.2
1JDW	-3.94	-5.57	-7.51	-8.24	-5.03	-5.52	-5.74	-6.18	-5.81	-6.14	-5.72	-5.89	-6.16	-5.52	-5.83	-5.7	-5.63	-5.73	-5.05	-5.47	-6.78	-6.32	-5.29
1JQE	-4.15	-5.89	-9	-11.3	-5.01	-4.77	-6.99	-7.28	-7.15	-7.63	-7.38	-7.69	-6.72	-6.55	-7.08	-7.24	-6.65	-7.07	-6.04	-6.79	-7.93	-6.2	-4.2
1JV1	-4.15	-6.45	-8.79	-10.2	-5.23	-6.63	-7.53	-6.98	-6.95	-6.78	-6.73	-7.33	-8.25	-6.69	-6.64	-6.82	-7.02	-6.58	-5.85	-7.3	-7.14	-6.44	-4.2
1K04	-3.04	-4.36	-7.24	-8.65	-3.96	-4.82	-5.28	-5.17	-5.42	-5.5	-5.49	-5.81	-5.73	-5.12	-5.3	-5.34	-4.92	-4.9	-5.78	-4.95	-5.79	-5.7	-4.67
1K3Y	-4.3	-5.65	-9.74	-11.3	-5.26	-5.74	-6.5	-6.68	-6.63	-7.03	-6.61	-7.17	-7.28	-6.09	-6.57	-6.81	-6.17	-5.87	-7.28	-6.08	-6.52	-5.3	-5.65
1KGD	-4.06	-4.94	-7.14	-8.22	-4.68	-5.62	-5.8	-5.67	-5.77	-5.69	-5.83	-5.72	-6.36	-5.18	-5.44	-5.62	-5.62	-5.43	-5.74	-5.64	-6.11	-6.55	-5.54

Table 2 (*Continued*).

	L1	L2	L3	L4	L7	L8	L9	L10	L11	L12	L13	L14	L15	L16	L17	L18	L19	L20	L21	L22	L23	L25	L26
1KWA	-3.94	-5.03	-6.94	-8.37	-4.18	-6.21	-5.8	-5.99	-6.12	-6.21	-6.03	-6.02	-7.49	-5.43	-5.58	-5.69	-5.49	-5.87	-5.78	-5.64	-6.47	-6.69	-5.35
1LS6	-4.4	-7	-11.8	-9.85	-4.97	-7.69	-7.86	-8.15	-7.88	-7.07	-8.1	-8.83	-9.61	-7.25	-7.88	-8.05	-7.32	-7.52	-5.69	-7.31	-7.49	-8.33	-7.34
1M9Z	-3.73	-4.78	-7.21	-8.64	-4.91	-4.86	-5.8	-5.52	-6.37	-5.8	-6.17	-6.28	-5.61	-5.49	-5.28	-5.2	-5.59	-5.74	-6.11	-5.62	-6.77	-6.88	-5.44
1MEO	-3.63	-4.54	-7.43	-8.15	-4.19	-5.17	-5.47	-5.67	-5.98	-5.75	-5.36	-5.97	-6.68	-5.29	-5.35	-5.6	-5.16	-5.38	-6.37	-5.73	-5.72	-5.97	-5.5
1MFG	-3.49	-5.73	-6.68	-7.75	-4.9	-5.75	-6.11	-6.64	-6.21	-5.94	-6.08	-6.55	-7.32	-5.82	-6.32	-6.48	-5.63	-5.72	-7.23	-5.64	-6.16	-6.15	-5.5
1MP8	-4.65	-5.21	-8.09	-8.24	-4.37	-5.43	-5.95	-5.9	-6.18	-5.81	-6.3	-6.03	-6.84	-5.4	-5.89	-6.01	-5.52	-5.88	-5.4	-5.79	-6.76	-5.93	-4.49
1MQ4	-4.47	-5.58	-8	-9.12	-4.76	-6.54	-6.54	-6.35	-6.56	-6.61	-6.62	-6.67	-8.04	-5.99	-6.21	-6.29	-6.33	-6.12	-6.2	-6.6	-6.1	-6.37	-5.96
1NB9	-4.16	-6.63	-9.69	-10.8	-5.56	-6.11	-7.38	-7.44	-7.43	-7.69	-8.66	-7.54	-7.38	-6.82	-6.81	-6.68	-6.92	-7.21	-5.29	-6.96	-7.86	-7.7	-6.92
1NM8	-5.07	-5.68	-8.48	-10.5	-4.49	-6.66	-7.67	-7.24	-7.18	-7.31	-6.73	-7.09	-7.69	-6.97	-7.1	-7.19	-7.09	-6.68	-6.74	-5.29	-5.96	-5.22	-4.47
1NN5	-3.64	-5.55	-9.55	-7.68	-4.88	-5.91	-6.63	-6.58	-6.88	-6.32	-7	-6.72	-6.71	-6.03	-6.19	-6.19	-6.19	-6.12	-5.24	-5.6	-7.19	-5.2	-5.77
1NTY	-4.13	-5.1	-6.8	-7.88	-3.9	-4.87	-5.47	-5.31	-5.6	-5.49	-5.38	-5.45	-5.77	-5.3	-5.44	-5.47	-5.57	-5.35	-6.12	-5.98	-8.86	-6.36	-6.1
1NUU	-4.42	-6.4	-8.62	-10.6	-5.3	-6.14	-6.85	-6.99	-6.89	-7.04	-7.31	-6.93	-7.63	-6.46	-6.61	-6.68	-6.6	-6.47	-6.26	-7.11	-6.7	-7.01	-7.32
1O4R	-3.67	-4.78	-6.38	-7.01	-4.65	-5.15	-5.07	-5.26	-5.19	-5.56	-5.44	-5.41	-6.6	-4.68	-4.97	-4.94	-4.98	-4.83	-6.4	-5.18	-5.68	-5.99	-5.16
1O6L	-4.89	-5.69	-8.36	-10.1	-5.06	-5.9	-6.08	-6.03	-6.18	-6.17	-6.17	-6.06	-6.63	-5.79	-5.92	-6	-6	-5.94	-6.31	-6.27	-6.5	-6.71	-5.46
1OTH	-3.67	-4.77	-6.43	-8.25	-5.69	-6.69	-6.51	-6.85	-6.47	-7.28	-7.03	-6.77	-8.06	-5.76	-5.44	-5.83	-6.02	-6.18	-5.02	-5.72	-11.7	-6.92	-5.33
1P4O	-4.71	-4.97	-7.51	-7.94	-4.81	-5.33	-6.59	-5.94	-6.03	-5.39	-6.11	-6.03	-6.39	-6.2	-6.04	-6.07	-6.59	-5.91	-5.87	-6.76	-6.67	-6.48	-13.8
1P5Z	-4.11	-5.48	-7.62	-9.11	-4.82	-5.41	-6.52	-6.25	-5.97	-6.37	-6.67	-6.32	-6.59	-5.94	-6.27	-6.4	-6.39	-5.64	-6.7	-6.1	-6.61	-6.42	-5.46
1PKX	-4.23	-5.63	-6.99	-8.63	-4.65	-6.12	-6.74	-6.78	-6.63	-6.16	-6.9	-5.79	-7.72	-5.94	-6.26	-6.38	-5.84	-6.52	-5.02	-5.45	-4.98	-6.82	-3.24
1QCF	-4.18	-6.14	-8.36	-8.94	-5.1	-5.77	-7.17	-7.45	-7.04	-6.6	-7.32	-7.02	-6.77	-6.41	-6.66	-6.74	-6.5	-6.04	-5.87	-6.2	-6.37	-6.2	-5.48
1QF8	-4.33	-6.88	-8.29	-10	-5.15	-6.47	-7.15	-7.03	-6.93	-7.47	-7.53	-7.29	-7.29	-6.78	-7.03	-7.19	-6.82	-6.49	-6.7	-6.16	-7.03	-6.1	-6.13

Table 3
Molecular docking results (docking scores in kcal/mol) of compounds in Table 1 at the hydrolases target (Class-III) (2 compounds could not derive a successful docking pose thus their docking scores are not tabulated). A color map is used for better visualization using certain threshold values of docking scores, such as derived docking scores values smaller than −9 kcal/mol were indicated with red color, values between −7 and −8 kcal/mol were colored with orange, values between −5 and −6 kcal/mol were given in yellow color and finally values greater than −5 kcal/mol were colored with gray.

	L1	L2	L3	L4	L5	L7	L8	L9	L10	L11	L12	L13	L14	L15	L16	L17	L18	L19	L20	L21	L22	L23	L24	L26
1A4I	-4.3	-6.3	-8	-9	-9.2	-4.8	-5	-6.2	-6	-6.5	-5.7	-6.5	-6.2	-5.8	-5.5	-5.6	-5.7	-5.9	-5.5	-5.7	-5.9	-5.9	-5.5	-5.2
1A6Q	-3.8	-5.7	-6.6	-7.2	-7.9	-4.5	-5.6	-6.1	-6.3	-6.2	-6.9	-6.2	-6.8	-6.5	-6.5	-6	-6.3	-6.4	-6.1	-6.1	-5.9	-6.6	-5.5	-6.2
1APY	-3.9	-5.9	-6.7	-8.3	-8.3	-4.6	-4.6	-6.1	-6	-5.9	-5.8	-6.7	-6.3	-5.7	-5.5	-5.6	-5.7	-5.3	-5.3	-5.5	-5.4	-5.9	-5	-4.9
1AYE	-4.6	-5.9	-8.2	-9.1	-9.5	-5.5	-5.4	-6.6	-6.7	-6.6	-7.1	-6.7	-7.1	-6.4	-6.4	-6.6	-6.7	-6.3	-6.9	-6.4	-6.9	-7.6	-6.2	-6.5
1B6A	-4.3	-7.2	-8.4	-10	-11	-4.9	-4.7	-6.3	-6.4	-6.3	-6.6	-6.9	-6.6	-5.7	-6.4	-6.6	-6.6	-6.2	-6.4	-6.2	-6.7	-6.3	-6	-6.7
1CS8	-4.5	-5.1	-7.7	-8.4	-7.9	-5.2	-5.3	-6.4	-6.1	-6.4	-6.1	-6.4	-6.4	-6.1	-6.1	-6.3	-6.3	-5.9	-5.6	-5.8	-5.7	-6.2	-5.4	-5.6
1CSB	-3.7	-5.3	-7.7	-8.8	-10	-4.8	-5.8	-6.7	-6.2	-6.2	-6.8	-6.5	-6.2	-5.8	-5.9	-6.1	-6.2	-6.3	-6	-6.3	-5.8	-6.5	-6	-5.7
1DEU	-2.2	-2.7	-4.7	-5.4	-5.7	-2.5	-2.8	-3.6	-3.9	-4.1	-3.8	-4	-3.7	-3.5	-3.8	-4	-4.1	-3.8	-3.5	-3.6	-4.2	-3.9	-3.6	-3.3
1DTD	-4.1	-5.3	-7	-8.6	-8.2	-4.6	-5.2	-6.3	-6.4	-6.4	-6.8	-6.4	-6.3	-6.4	-6.3	-6.5	-6.6	-6	-6.7	-6	-6	-7.1	-5.9	-6
1EDM	-3.3	-4.8	-7.1	-8	-8.4	-4.2	-3.9	-5.5	-5.6	-5.8	-5.7	-6.3	-5.8	-4.8	-5.3	-5.6	-5.8	-5.2	-5.2	-5.6	-5.6	-5.6	-5.6	-5.2
1ELV	-4.6	-6.2	-8.1	-8.3	-8.8	-5.6	-5.9	-6.6	-7.6	-7.1	-6.8	-6.9	-6.1	-7.3	-6.3	-7	-7.1	-5.9	-6.7	-6	-6.5	-6.3	-6	-6.1
1F3U	-3.6	-4.8	-7	-7.9	-8.2	-4.4	-4.7	-5.5	-5.6	-5.8	-5.9	-6	-5.8	-5.7	-5.2	-5.3	-5.4	-5.5	-6	-5.4	-5.9	-6.6	-6	-6
1FH0	-2.7	-2.8	-4.4	-5.5	-4.9	-2.4	-4.2	-3.7	-3.5	-3.8	-3.5	-3.5	-3.8	-5	-3.6	-3.7	-3.7	-3.9	-3.5	-3.8	-3.6	-4.2	-3.5	-3.6
1FIT	-3.9	-5.5	-8.6	-10	-10	-4	-6.2	-6.5	-6.4	-6.6	-6.1	-6	-6.3	-6.9	-6	-6.2	-6.2	-5.9	-5.9	-6.2	-5.5	-6.1	-5.4	-5.6
1FJ2	-4.9	-7.2	-7.5	-8.7	-8.9	-5.6	-5.1	-6.7	-7.2	-7.4	-6.8	-6.6	-7.2	-6	-6.4	-6.6	-6.7	-6.2	-6.5	-6.7	-6.4	-6.6	-5.7	-6.4
1FO3	-3.6	-4.8	-7	-7.9	-8.2	-4.4	-4.7	-5.5	-5.6	-5.8	-5.9	-6	-5.8	-5.7	-5.2	-5.3	-5.4	-5.5	-6	-5.4	-5.9	-6.6	-6	-6
1FPZ	-3.2	-4.3	-6.5	-7.6	-8.1	-3.7	-5.6	-5.4	-5.1	-5.3	-5.3	-5.6	-5.6	-6	-5	-5.1	-5.1	-5.1	-4.7	-5.1	-4.6	-5.3	-4.4	-4.2
1GQV	-3.7	-4.5	-7.2	-8.2	-8.2	-4.6	-5.9	-5.9	-5.7	-5.2	-5.8	-5.7	-5.6	-7.4	-5.2	-5.3	-5.3	-5.3	-5.2	-5	-5.3	-5.5	-5.6	-5
1H7S	-4.1	-5.1	-7	-8.6	-9	-4.8	-5.5	-6	-6.1	-5.8	-6	-5.8	-5.9	-7.1	-5.9	-6.2	-6.4	-5.8	-5.9	-5.9	-6	-6.4	-5.7	-6
1HAZ	-4.5	-4.9	-7	-8.4	-9.2	-5.7	-5.6	-6	-5.6	-5.5	-5.7	-5.9	-5.4	-6.6	-5.3	-5.3	-5.4	-5.6	-5.7	-5.7	-5.8	-6.3	-5.4	-5.9
1HDK	-3.6	-4.3	-6.1	-7.1	-7.5	-4	-4.5	-5.3	-5.3	-5	-5	-5.8	-5.4	-5.3	-4.7	-5	-5	-4.8	-5	-5.6	-5.3	-5.7	-5.4	-5.2
1HFC	-4.7	-6.3	-7.2	-8.3	-8.4	-5.5	-5.3	-6.5	-6.3	-6.3	-6.3	-6.3	-6.5	-5.5	-6.5	-6.4	-6.4	-6.3	-6.2	-6.3	-6.3	-6.4	-5.9	-5.6
1HKK	-4.2	-5.6	-8.6	-10	-11	-5.1	-4.9	-6.2	-6.4	-6.5	-6.7	-6.3	-6.6	-5.6	-5.8	-6.1	-6.2	-6	-6.4	-6.4	-6.2	-7	-5.7	-5.7
1HTR	-4.4	-6.2	-7.6	-9.8	-10	-4.6	-4.8	-6.5	-6.9	-7	-7.1	-6.7	-7	-6.3	-6.3	-6.4	-6.5	-6	-6.3	-6.7	-6.5	-6.7	-5.8	-6.5
1HY7	-4.4	-6.3	-8.9	-9.6	-9.3	-4.8	-5.5	-7.9	-8.3	-7.9	-8.2	-7.5	-8.2	-6.7	-7.7	-8.1	-8.2	-7.6	-8.2	-7.5	-7.6	-8.3	-7.2	-8
1I71	-3.3	-4.3	-6.6	-7.6	-7.7	-4.2	-4.5	-5	-5.1	-5.3	-5.2	-5.4	-5.3	-5.7	-4.9	-5	-5	-5	-5.1	-4.8	-4.8	-5.7	-4.7	-4.8

Table 3 (*Continued*).

	L1	L2	L3	L4	L5	L7	L8	L9	L10	L11	L12	L13	L14	L15	L16	L17	L18	L19	L20	L21	L22	L23	L24	L26
1I76	-4.8	-6.7	-7.6	-9.6	-9.3	-4.8	-6	-7.7	-8.4	-8.1	-8	-7.1	-8.4	-7.3	-7.7	-7.9	-7.9	-7.6	-8.3	-7.6	-7.5	-8.4	-7.3	-8.1
1ITU	-4.4	-5.5	-7.7	-9	-9	-5.3	-5.9	-6.6	-6.5	-6.4	-6.9	-7.1	-6.6	-6.8	-6.1	-6.3	-6.4	-6.1	-6.3	-6.2	-6.6	-6.8	-6.2	-6.6
1ITV	-5	-6.4	-7.5	-9.2	-9.8	-4.9	-6.2	-7.1	-7.9	-7.2	-8.1	-6.5	-7.5	-8	-7	-7.3	-7.4	-6.7	-7.1	-7.3	-7.1	-7.5	-6.9	-7
1J8F	-3.6	-5.3	-6.6	-8.2	-8.1	-5	-4	-5.7	-6.3	-6.7	-5.4	-5.7	-5.9	-6.2	-5.5	-5.5	-5.6	-5.6	-6	-5.5	-5.5	-6.4	-5.4	-5.6
1JSF	-3.7	-5.8	-7.4	-7.9	-8.7	-4.4	-5.1	-5.8	-5.8	-6.2	-5.9	-5.9	-6.8	-6	-5.6	-5.7	-5.7	-5.6	-5.2	-5.9	-5.8	-5.7	-5.8	-5.3
1JY1	-4.2	-6.7	-8	-9.8	-9.3	-4.7	-6.6	-6	-7.7	-7.3	-6.9	-6	-7.3	-8	-6.8	-7.3	-7.5	-6.8	-7	-6.2	-6.6	-7.5	-6.5	-6.7
1KI0	-4.3	-6	-7.2	-8.8	-9	-4.9	-5.6	-6.2	-6.5	-6.5	-6.3	-6.4	-5.8	-6.6	-5.8	-5.9	-6	-6.1	-5.9	-6.2	-5.9	-6.3	-5.9	-5.5
1KRN	-4.2	-5.3	-6.6	-8.5	-8.5	-4.3	-5.8	-5.5	-5.2	-5.7	-5.2	-6.1	-5.9	-6.3	-5.1	-5.2	-5	-5.1	-4.9	-5.1	-5.1	-5.7	-5	-5
1KWM	-3.8	-4.9	-6.4	-7.8	-7.7	-4.4	-5.3	-5.5	-5.4	-5.6	-5.6	-5.3	-5.5	-5.8	-5	-5.5	-5.7	-5.4	-5.1	-5	-5.1	-5.6	-5.1	-5.4
1L9X	-4.1	-6	-7.1	-7.8	-8.5	-4.7	-6.2	-5.9	-6.8	-5.9	-6.2	-6.2	-6.7	-6.8	-6.1	-6.5	-6.4	-6.3	-6.6	-7.1	-6.5	-6.3	-5.5	-5.6
1LAR	-3.9	-4.7	-7.1	-8.1	-9	-4.7	-5.1	-5.7	-5.9	-5.6	-6.5	-5.8	-6	-6.7	-5.2	-5.4	-5.7	-5.4	-5.8	-5.2	-5.4	-6	-5.2	-5.6
1LCF	-4.2	-6	-7.7	-9.7	-9.3	-5.2	-5.9	-6.7	-6.9	-6.4	-6.9	-7.1	-6.8	-7.5	-5.8	-6.4	-6.5	-6.5	-6.6	-6.5	-5.9	-7.1	-6.3	-5.9
1LCY	-4.4	-6	-7.6	-8.9	-9.9	-4.7	-5.8	-6.9	-7.2	-7.3	-7.2	-7.4	-7.5	-7	-6.8	-6.9	-7	-7.2	-6.9	-6.8	-6.9	-7.1	-6.3	-6.3
1LE6	-4	-5.5	-9.1	-10	-11	-4.4	-5.4	-6.8	-7	-7.3	-7.3	-7.2	-7	-6.8	-6.4	-6.7	-6.8	-6.2	-6.3	-6.9	-6.3	-7.3	-5.5	-5.8
1LO6	-4	-5.3	-7.5	-8.8	-9.3	-4.7	-5.7	-7	-6.6	-6.5	-6.4	-6.7	-6.2	-7	-6	-6.2	-6.1	-6.1	-6	-6.2	-6.2	-6.6	-5.8	-5.8
1LQV	-3.6	-6.2	-7.5	-8.4	-8.9	-4.1	-6.6	-6.9	-7.4	-7.1	-7.5	-7.1	-7.2	-7.8	-6.8	-7.4	-7.6	-6.6	-6.5	-6.5	-6.4	-6.9	-5.8	-5.8
1M6D	-4.7	-5.6	-9.1	-8.8	-9	-4.6	-5.1	-6.7	-7.1	-6.8	-7	-6.9	-7.5	-6.6	-6.3	-6.8	-6.7	-6.1	-6.5	-5.9	-6	-6.9	-5.7	-6.1
1MHW	-5.6	-5.2	-8.3	-8.9	-9.4	-4.6	-5	-6.1	-5.8	-6.2	-6.2	-6.4	-5.9	-5.5	-5.4	-5.5	-5.9	-5.8	-5.7	-5.7	-5.9	-6.3	-6	-6
1NE7	-4.1	-5.7	-8.1	-9.9	-9.4	-5.3	-6.3	-6.4	-6.9	-6.3	-6.6	-6	-6.6	-7.4	-5.9	-5.8	-6.5	-5.7	-6.4	-5.6	-5.7	-6.5	-5.7	-5.9
1NNL	-3.6	-4.9	-6.6	-7.8	-8.3	-4.5	-6.2	-5.9	-5.9	-5.9	-6	-6.1	-6.1	-7.3	-5.5	-5.6	-5.7	-6	-5.6	-5.8	-5.7	-6.5	-5.8	-5.3
1NZI	-4.2	-5.8	-7.6	-8.7	-9	-4.5	-3.8	-6	-6.4	-6.1	-6.1	-5.9	-6.3	-4.9	-6	-6.3	-6.1	-5.6	-6	-5.7	-5.7	-6.2	-5.3	-5.4

Table 4
Molecular docking results (docking scores in kcal/mol) of compounds in Table 1 at the Lyases target (Class-IV) (9 compounds could not derive a successful docking pose thus their docking scores are not tabulated). A color map is used for better visualization using certain threshold values of docking scores, such as derived docking scores values smaller than −9 kcal/mol were indicated with red color, values between −7 and −8 kcal/mol were colored with orange, values between −5 and −6 kcal/mol were given in yellow color and finally values greater than −5 kcal/mol were colored with gray.

	L1	L3	L5	L7	L9	L10	L11	L12	L15	L19	L22	L23	L24	L25	L26
1ALD	-4.62	-7.85	-9.48	-5.01	-6.04	-6	-6.32	-6.05	-6.7	-6.04	-5.7	-6.31	-5.45	-6.41	-5.67
1HCB	-3.84	-6.62	-9.13	-4.33	-6.17	-6.1	-6.43	-5.96	-6.68	-5.8	-5.55	-6.43	-5.46	-6.26	-5.93
1IKT	-4.41	-8.67	-9.86	-4.4	-6.74	-7.21	-7.23	-7	-7.84	-6.17	-6.35	-6.48	-5.67	-7.26	-5.75
1JD0	-4.51	-8.62	-11.4	-4.66	-6.92	-7.32	-7.15	-7.21		-6.7	-6.86	-7.52	-6.7	-7.42	-6.6
1JL0	-4.37	-6.58	-8.49	-4.66	-5.67	-5.28	-5.87	-5.28		-5.58	-5.33	-6.09	-5.17	-6.48	-5.19
1JR2	-4.27	-6.89	-8.96	-4.68	-5.41	-5.82	-5.79	-6.34		-5.28	-5.44	-6.18	-5.37	-6.53	-5.5
1KHB	-4.7	-8.76	-8.32	-5.45	-7	-6.78	-7.12	-7.19		-7.02	-7.05	-7.12	-6.88	-6.87	-6.06
1R3S	-4.5	-9	-11.2	-4.52	-7.3	-7.49	-7.44	-7.69	-8.3	-6.63	-6.88	-7.05	-6.56	-6.82	-6.73
1T2A	-3.93	-8.93	-10.5	-5.05	-6.35	-6.31				-6.36	-6.49	-6.85	-6.68	-6.49	-6.09
2AKZ	-3.78	-7.05	-9.3	-5.16	-5.59	-5.99				-5.31	-5.63	-6.43	-5.21	-6.08	-5.38
2B3Y	-3.8	-8.96	-10.9	-4.32	-6.21	-6.95				-5.75	-5.92	-6.25	-5.7	-6.86	-5.91
2B69	-4.55	-8.55	-10.9	-5.38	-6.69	-6.79	-6.45	-7.23	-7.21	-6.46	-6.42	-6.44	-5.97	-7.28	-6.03
2J91	-4.39	-8.38	-9.62	-5.46	-6.56	-6.94				-6.61	-6.77	-6.76	-6.28	-6.68	-6.57
2JIS	-4.25	-7.35	-9.68	-4.63	-5.92	-6.12				-6	-5.7	-6.32	-5.41	-6.81	-5.6
2O3H	-4.18	-7.68	-9.17	-4.82	-6.16	-6	-6.1	-5.92	-6.19	-5.89	-5.5	-6.54	-5.81	-6.21	-5.81
2OO0	-4.36	-8.75	-10.4	-4.89	-7.35	-6.75				-6.63	-6.76	-7.67	-6.63	-6.91	-6.95
2W2J	-4.95	-8.12	-10.3	-4.96	-6.61	-6.51	-6.25	-7.05	-5.97	-5.8	-5.94	-6.72	-5.56	-6.49	-6.09
2WZ1	-5.42	-7.99	-10.2	-5.4	-6.54	-6.82	-7.22	-7.05	-7.44	-6.66	-6.44	-7.55	-6.13	-8.02	-6.56
2XSX	-3.92	-6.61	-8.5	-4.4	-6.03	-6.54				-5.92	-5.92	-6.45	-5.92	-6.64	-6.04
3AQI	-4.97	-8.72	-10.4	-4.98	-7.78	-9.21				-8.14	-7.55	-8.92	-6.39	-8.78	-7.86
3COG	-5.37	-8.25	-8.71	-5.47	-6.11	-5.54				-5.24	-5.77	-6.22	-5.27	-6.38	-5.69
3D0N	-5.62	-9.28	-10.4	-5.62	-6.54	-6.27	-6.56	-6.7		-6.16	-5.74	-6.73	-6.01	-6.48	-6.09
3EO4	-4.9	-7.88	-5.93	-4.9	-6.29	-6.2				-5.81	-5.89	-7.24	-5.92	-6.78	-5.76
3EP6	-4.79	-8.84	-10.7	-4.8	-7.01	-7.11	-7.01	-7.34	-6.56	-6.68	-6.72	-6.8	-6.22	-7.38	-6.45
3EWY	-4.69	-6.76	-7.55	-4.69	-5.62	-6.32	-5.65	-5.99	-6.47	-5.72	-5.8	-6.56	-5.55	-6.89	-5.79
3FE4	-4.86	-7.85	-10.2	-4.86	-6.63	-6.84	-6.81	-7.01		-6.06	-6.33	-6.45	-6.1	-6.65	-6.38
3FVS	-4.74	-10.6	-11.7	-4.74	-6.92	-7.15				-6.39	-6.39	-7.47	-6.01	-7.12	-6.3
3FW3	-4.57	-8.56	-9.38	-4.64	-6.61	-6.69	-6.57	-7.24		-6.34	-6.31	-6.84	-6.42	-6.69	-6.26
3IR3	-4.8	-8.8	-9.91	-4.79	-7.06	-6.67	-6.81	-6.84	-7.4	-6.44	-6.79	-7.12	-6.04	-6.88	-5.95
3KAN	-4.65	-7.9	-10.1	-4.65	-6.61	-6.67	-6.37	-6.23	-7.8	-6.29	-6.22	-6.5	-6.03	-6.27	-5.47
3KS3	-4.97	-7.37	-9.29	-4.97	-5.92	-6.27	-6.12	-6.56	-6.81	-5.87	-5.86	-6.83	-5.67	-6.64	-5.31
3L6B	-3.9	-7.85	-8.53	-5.31	-5.92	-6.32	-6.44	-6.23	-5.99	-5.92	-6.24	-6.35	-5.81	-6.73	-5.74
3PCV	-3.21	-7.11	-8.18	-3.9	-5.51	-5.77	-5.78	-5.78	-6.34	-5.1	-4.85	-5.46	-4.62	-5.68	-4.93
3S5O	-3.98	-7.28	-9.49	-4.84	-5.99	-6.2	-6.57	-6.33	-6.16	-6.25	-6.33	-6	-5.89	-6.29	-6.24
3UYQ	-4.46	-7.57	-8.82	-4.38	-6.12	-5.94	-5.95	-6.06	-6.36	-6.11	-6.14	-6.27	-6.04	-6.29	-6.33
3VW9	-4.39	-8.53	-9.41	-4.8	-6.59	-6.61	-6.67	-7.14	-6.9	-7.09	-6.75	-7.67	-6.14	-7.22	-6.12
4E1O	-3.39	-8.07	-10.2		-6.3	-6.52				-5.7	-6.08	-6.53	-5.76	-6.62	-6.05
4H27	-3.79	-8.45	-9.87	-4.87	-6.82	-6.62	-7.18	-7.16	-7.9	-5.97	-5.78	-6.37	-5.65	-6.25	-5.61

Table 4 (*Continued*).

	L1	L3	L4	L5	L6	L8	L9	L10	L11	L12	L13	L14	L15	L16	L17	L18	L19	L20	L21	L22	L23	L24	L25	L26
1C9H	-4	-6.5	-9.4	-9.9	-5.2	-5.9	-6.6	-6.5	-6.5	-5.9	-6.1	-5.5	-5.8	-6.4	-6.2	-6.3	-6.6	-5.9	-6	-6.3	-6.2	-5.7	-5.8	-5.4
1EK6	-3.9	-8.9	-9.1	-10	-6.6	-6.2	-7	-6.8	-7	-7	-7.2	-7.4	-7.5	-6.3	-6.7	-6.8	-6.7	-6.7	-6.4	-6.6	-7.7	-6.4	-7.4	-6.3
1FW1	-3.9	-7.4	-9	-9.5	-6.2	-6.2	-5.9	-5.9	-5.9	-5.7	-6.3	-5.8	-7	-5.2	-5.5	-5.6	-5.3	-5.6	-5.5	-5.7	-6.6	-5.6	-6	-5.5
1IAT	-4.2	-7.6	-8.8	-8.9	-5.7	-5.5	-6	-6.2	-6.3	-6	-6.4	-6.2	-7.1	-5.7	-5.8	-6.1	-5.7	-5.6	-5.6	-5.9	-6.1	-5.6	-6.3	-5.9
1Q1C	-4	-7.5	-9.2	-9.8	-5.2	-5.3	-6.3	-6.3	-6.5	-6.1	-5.9	-6.7	-5.9	-6	-6.2	-6.3	-6.7	-6.2	-6.3	-5.9	-6.9	-6	-7.1	-6.3
1QOI	-3.6	-7	-7.9	-8	-5.1	-4.8	-5.1	-5.3	-5.5	-5.5	-5.4	-5.2	-6	-5	-5.4	-5.6	-5.1	-5.4	-5.2	-5.2	-5.6	-5	-5.7	-5.1
1SG4	-4.2	-8.2	-9.2	-9.8	-6.7	-6	-7.3	-8.1	-7.5	-8.5	-7.3	-7.8	-8.2	-6.9	-7.3	-7.4	-7	-7	-7.2	-6.7	-7.3	-6.3	-8.1	-6.5
1ZKC	-3.8	-7.1	-7.9	-8.3	-5.4	-6.6	-5.9	-6.8	-6.8	-5.6	-6	-6.4	-7.7	-5.7	-5.8	-5.9	-5.7	-6.2	-6.4	-5.7	-6.4	-5.3	-6.6	-5.4
1ZXM	-4.4	-7.4	-9.3	-10	-7.1	-6.5	-6.9	-7.1	-7.1	-6.8	-7.6	-6.8	-7.5	-6.4	-6.8	-6.5	-6.5	-6.4	-5.7	-6.6	-6.4	-6.1	-6.3	-6.3
2A2N	-4.1	-7.6	-8.8	-9.9	-5.2	-5.1	-6	-6	-6.2	-6.2	-6.1	-6.3	-6.6	-5.6	-6.1	-6.2	-5.3	-5.9	-5.6	-5.8	-6.4	-5.7	-7.1	-5.9
2CVD	-4	-7.8	-10	-9.9	-5.6	-5.2	-6.4	-6.6	-6.7	-6.5	-6.5	-6.5	-6.2	-6.1	-6.5	-6.6	-6.1	-6.2	-6.4	-5.9	-6.4	-6.1	-6.8	-5.8
2DHO	-4	-7.8	-9.2	-8.9	-4.8	-5.2	-5.8	-5.6	-5.7	-5.8	-5.8	-5.9	-6.7	-5.2	-5.5	-5.5	-5.3	-5.3	-5.6	-5.1	-5.6	-5.1	-6.2	-5.1
2ESL	-4.6	-9	-10	-8.8	-5.9	-5.9	-7.1	-7.3	-6.8	-7.4	-7.1	-7.3	-6.8	-6.7	-7.2	-7.3	-7	-6.9	-7.2	-7.2	-6.8	-6.7	-7.8	-7.1
2F6Q	-4.3	-7.3	-9.1	-10	-6.4	-6.8	-7.7	-7.9	-8.1	-7.7	-8.1	-6.3	-7.3	-7.2	-7.2	-7	-7.1	-7.8	-7.7	-7.1	-8.2	-6.7	-8.6	-7.5
2FUE	-4.1	-6.7	-7.8	-8.3	-4.9	-5.9	-5.9	-5.7	-5.4	-5.6	-6	-5.4	-6.2	-5.6	-5.5	-5.5	-5.8	-5.7	-5.7	-5.4	-6.1	-5.1	-6.1	-5.9
2G62	-3.8	-6.9	-8.1	-8.7	-5.1	-5.2	-5.3	-5.6	-5.6	-5.5	-6.1	-6.3	-6.4	-5.1	-5.2	-5.5	-5.6	-5.8	-5.8	-5.3	-6.4	-5.5	-6.5	-5.6
2H8L	-4.4	-9	-9.8	-9.9	-5.4	-6	-7.5	-7.8	-6.8	-7.3	-7.2	-7.3	-7	-7.1	-7.5	-7.4	-6.4	-7.2	-6.7	-7.1	-7.1	-6.7	-7.3	-7.1
2HE9	-4.4	-6.4	-8.1	-7.7	-5.6	-6.3	-6.3	-6.8	-6.2	-6.1	-6.3	-6.3	-7.3	-6.1	-6.3	-6.2	-6	-6.5	-6.4	-6.4	-6.3	-6	-7	-6.2
2HHJ	-4.2	-8	-8.9	-9.3	-5.3	-6.9	-7.8	-7.5	-9.1	-7.2	-7.5	-7.3	-7.3	-8.2	-7.3	-7.4	-8.1	-8	-8.6	-9	-8.7	-8.7	-8.9	-8.5
2HQ6	-3.9	-6.7	-8.1	-9	-4.9	-4.8	-5.6	-5.4	-5.6	-5.6	-5.5	-5.5	-5.6	-5.2	-5.3	-5.4	-5.4	-5.4	-5.1	-5.2	-6.1	-5.6	-6.3	-5.3
2JK2	-3.7	-7.2	-8.1	-8	-5.9	-5.3	-6.1	-6.2	-6	-5.9	-6.5	-6	-6.1	-5.8	-6	-6.1	-6.5	-6.9	-6.5	-6.2	-8	-6	-7.6	-6.3
2OK3	-4.2	-6.8	-7.7	-8.1	-5	-4.9	-5.4	-5.9	-6.3	-5.7	-5.4	-5.4	-5.9	-5.3	-5.7	-5.9	-5.3	-5.2	-5.8	-5.7	-5.6	-5.6	-6.5	-5.1
2PBC	-4.3	-8.4	-10	-11	-5.3	-5.6	-6.5	-6.1	-5.9	-6.4	-6.8	-6.1	-7	-5.9	-6	-6	-6	-5.8	-5.6	-5.7	-6.3	-5.7	-6.8	-5.5
2PNY	-4.5	-7	-8.4	-8.8	-4.4	-4.8	-5.4	-5.8	-5.3	-5.6	-5.8	-5.6	-5.6	-5.4	-5.7	-5.8	-5.1	-5.2	-5.2	-5.5	-6.3	-5.3	-6.3	-5.1
2PPN	-4.1	-7.1	-8.7	-9.7	-4.8	-5	-5.8	-5.2	-5.6	-5.6	-5.9	-5.5	-6	-5.4	-5.3	-5.4	-5.6	-5.2	-5.7	-5.7	-5.8	-5.3	-5.9	-5.2
2R99	-4.1	-6.9	-7.9	-8.8	-5.5	-6	-6	-5.7	-5.8	-6.1	-6.3	-6.2	-7.1	-5.3	-5.7	-5.8	-5.6	-5.3	-5.6	-5.6	-6	-5.7	-6	-5.2
2V9K	-3.6	-7.2	-8.7	-8.1	-5.2	-5.5	-5.6	-6.2	-5.7	-7	-5.9	-6.9	-6.5	-5.1	-5.5	-5.6	-5.6	-5.7	-5.5	-5.5	-6.6	-5.6	-6.8	-5.3

Table 5
Molecular docking results (docking scores in kcal/mol) of compounds in Table 1at the isomerase enzymes (Class-V) (2 compounds could not derive a successful docking pose thus their docking scores are not tabulated). A color map is used for better visualization using certain threshold values of docking scores, such as derived docking scores values smaller than −9 kcal/mol were indicated with red color, values between −7 and −8 kcal/mol were colored with orange, values between −5 and −6 kcal/mol were given in yellow color and finally values greater than −5 kcal/mol were colored with gray.

	L1	L3	L4	L5	L6	L8	L9	L10	L11	L12	L13	L14	L15	L16	L17	L18	L19	L20	L21	L22	L23	L24	L25	L26
2VRE	-4	-8	-9	-10	-5.3	-6.2	-7.1	-7.2	-7.3	-7.5	-7.2	-7.9	-7.5	-6.5	-7.1	-7.3	-6.3	-6.6	-6.5	-6.1	-7	-5.7	-7.6	-5.9
2WFI	-4.2	-7.6	-9.1	-8.5	-5.8	-5.2	-6.2	-6.7	-6.7	-7	-6.4	-7	-6.8	-6.1	-6.4	-6.4	-6.2	-6.6	-6.3	-5.8	-6.3	-5.7	-6.7	-6.1
2X25	-3.8	-6.8	-8.2	-8.8	-5.3	-5.6	-5.3	-5.7	-5.4	-5.8	-5.8	-5.8	-6.6	-5.1	-5.5	-5.6	-5.3	-5.5	-5.5	-5.4	-6.4	-5	-6.6	-5.1
2X7K	-4.1	-6.8	-8.6	-9.3	-5.3	-5.4	-5.9	-6	-6	-6.4	-5.9	-6.1	-7.1	-5.4	-5.8	-5.8	-5.5	-5.8	-5.7	-5.5	-5.9	-5.3	-6.9	-5.5
2XIJ	-4.2	-8.9	-10	-11	-5.7	-5.8	-7.3	-7.3	-6.9	-7.6	-7.1	-7.3	-7.5	-6.8	-7.2	-7.4	-6.6	-6.4	-6.5	-6.5	-6.9	-6.3	-7.1	-6.2
3B6H	-3.8	-8.3	-9.8	-10	-5.6	-5.5	-6.3	-6.2	-6.6	-7.6	-6.4	-6.2	-6.8	-5.8	-6.3	-6.4	-5.7	-5.7	-5.5	-5.6	-5.9	-5.7	-6.3	-5.9
3EY6	-3.9	-7.6	-8.5	-8.9	-4.5	-4.8	-5.6	-5.2	-5.2	-5.4	-5.7	-5.1	-6	-4.9	-5.2	-5.4	-5.3	-5.1	-5	-5.6	-6.2	-5.2	-5.9	-5.2
3I6C	-3.4	-7	-8.3	-8.8	-4.6	-5.2	-5.6	-5.5	-6.1	-5.6	-5.6	-5.8	-6.6	-5.4	-5.5	-5.6	-5.8	-5.6	-5.5	-5.6	-6.3	-5.2	-6.6	-5.1
3ICH	-3.6	-6.4	-7.5	-8.1	-5.3	-5.8	-5.5	-6	-5.7	-6	-5.6	-5.6	-7.2	-5.5	-5.8	-5.9	-5.5	-5.6	-5.6	-5.2	-6.2	-5.4	-6	-5.5
3IDV	-3.8	-7.7	-8.6	-9.2	-5.5	-5.3	-6.7	-6.4	-6.1	-6	-6.8	-6.2	-7.2	-6	-6.1	-5.9	-6.6	-6.1	-6.3	-5.9	-7.5	-6.6	-6.8	-6.2
3IJJ	-4.5	-7.9	-9.7	-9.3	-5.6	-7.9	-6.1	-6.7	-6.6	-6.2	-6.1	-6.6	-9.1	-6.3	-6.7	-6.8	-5.9	-5.9	-6.1	-5.6	-6.1	-5.6	-6.5	-5.6
3L6B	-4	-7.8	-8.1	-8.4	-6.1	-6.2	-5.9	-6.4	-6.4	-6.2	-6.1	-6.3	-6	-6	-6.5	-6.6	-5.9	-6.2	-6.3	-6.2	-6.4	-5.8	-6.7	-5.8
3MDF	-3.9	-7.3	-8.2	-8.3	-4.7	-4.4	-5.5	-5.6	-5.3	-5.8	-5.4	-5.4	-5.1	-4.9	-5.2	-5.2	-5.2	-5.5	-5.2	-5.3	-6.1	-5.1	-6.3	-5
3O22	-4	-7.8	-9.4	-9.1	-5.5	-7.1	-6.6	-6.8	-7.1	-6.7	-6.8	-7.2	-8	-6.6	-6.9	-7	-6.5	-6.5	-6.7	-6.6	-6.8	-6.2	-7.1	-6.3
3O5E	-4.1	-7.4	-8.9	-9.5	-5.1	-5.9	-6.1	-6	-5.8	-5.6	-5.8	-5.8	-6.9	-5.7	-5.8	-5.9	-5.7	-5.6	-5.5	-6.1	-6	-5.7	-6.2	-5.7
3O5Q	-4.5	-7.9	-9.7	-11	-4.9	-5.9	-6.2	-5.5	-5.5	-5.7	-6.3	-5.8	-6.6	-5.4	-5.3	-5.4	-5.7	-5.2	-5.4	-5.7	-5.8	-5.6	-6.3	-5.1
3OVP	-3.6	-7.7	-8.8	-8.8	-5	-4.2	-6.4	-6.4	-6	-6.5	-6.2	-6.4	-4.8	-5.5	-5.9	-6.1	-5.8	-6	-5.8	-6	-6.4	-5.6	-6.7	-6.4
3PH9	-4.1	-8	-8.7	-8.9	-4.7	-4.7	-5.3	-5.6	-5.7	-5.6	-5.7	-5.5	-6.2	-5	-5.1	-5.3	-5.1	-5.4	-5.3	-5	-5.8	-5.3	-6.4	-5.5
3RCG	-3.8	-6.7	-8.4	-9.4	-5.4	-5.3	-5.3	-5.4	-5.6	-5.4	-5.3	-5.2	-6.1	-5.1	-5.5	-5.6	-5	-5.6	-5.7	-5.4	-5.5	-5	-5.8	-5
3RMU	-4.1	-8	-9.3	-9.9	-5.4	-5.3	-7	-6.7	-6.3	-7.2	-6.9	-6.1	-6.2	-6.2	-6.5	-6.4	-6.7	-6.1	-6.1	-6.2	-6.8	-6.3	-6.5	-5.8
3TC5	-3.5	-6.6	-7.9	-8.5	-5.5	-5.5	-5.7	-5.6	-5.8	-5.7	-5.8	-5.8	-6.6	-5.1	-5.4	-5.5	-5.5	-5.3	-5.3	-5.5	-6.2	-5.4	-6.5	-5.5
3UI4	-4.1	-7.3	-9	-8.2	-4.8	-5	-5.7	-5.8	-5.5	-5.9	-5.8	-5.7	-6.3	-5.1	-5.3	-5.4	-5.2	-5.5	-5.3	-5.6	-6.1	-5.1	-6.2	-5.1
3UVT	-4.2	-8	-8.7	-8.6	-5.4	-5.4	-6	-6.3	-6.1	-6.2	-6.1	-6.1	-6.6	-5.8	-6.1	-6.2	-5.7	-6	-5.6	-6.4	-6.2	-5.7	-6.3	-5.9
4A35	-4.7	-7.7	-8.1	-8.4	-5.4	-5	-6.2	-6	-6.2	-6.2	-6.2	-6	-5.7	-5.6	-5.7	-5.7	-6.1	-5.5	-6.1	-5.9	-6.4	-5.4	-6.1	-5.7

Table 6
Molecular docking results (docking scores in kcal/mol) of compounds in Table 1at the ligaseses (Class-VI) (6 compounds could not derive a successful docking pose thus their docking scores are not tabulated). A color map is used for better visualization using certain threshold values of docking scores, such as derived docking scores values smaller than −9 kcal/mol were indicated with red color, values between −7 and −8 kcal/mol were colored with orange, values between −5 and −6 kcal/mol were given in yellow color and finally values greater than −5 kcal/mol were colored with gray.

	L1	L2	L4	L5	L7	L8	L9	L10	L11	L12	L13	L14	L15	L16	L17	L18	L19	L22	L23	L24
1I2T	-3.09	-3.71	-7.57	-7.82	-3.59	-4.71	-4.49	-4.37	-5.15	-4.5	-4.48	-5.28	-5.29	-4.34	-4.51	-4.56	-4.48	-4.42	-5.64	-4.41
1I7K	-4.13	-5.62	-9.01	-9.11	-4.12	-5.6	-6.3	-6.54	-6.13	-6.14	-6.18	-6.14	-6.36	-5.6	-5.76	-5.87	-5.87	-5.49	-6.92	-5.4
1LB6	-3.78	-5.1	-8.38	-8.38	-4.14	-4.66	-5.22	-5.41	-5.21	-5.41	-5.78	-5.62	-5.76	-4.95	-5.08	-5.19	-5.29	-5.18	-5.61	-5.18
1LGP	-3.58	-5.4	-10.3	-11.3	-4.03	-5.86	-6.55	-6.7	-6.47	-6.91	-6.74	-6.89	-7.34	-5.87	-6.31	-6.45	-6.05	-6.33	-6.62	-5.84
1N3L	-4.03	-5.41	-10.4	-9.79	-4.59	-5.92	-6.62	-6.64	-6.56	-6.9	-5.85	-6.44	-7.36	-6.29	-6.69	-6.79	-6.08	-6.69	-6.61	-5.72
1T15	-3.66	-5.16	-9.12	-9.28	-4.53	-6.24	-5.49	-6.06	-5.76	-5.77	-5.74	-5.79	-7.58	-5.31	-5.63	-5.75	-5.68	-5.7	-6.18	-6.01
1Y02	-3.18	-4.52	-7.75	-7.78	-4.19	-5.28	-5.95	-5.67	-5.36	-5.76	-6.2	-6.03	-6.17	-5.1	-5.09	-5.12	-4.92	-5.35	-5.74	-5
1Y6L	-4.09	-5.38	-8.21	-8.69	-4.51	-5.99	-6.29	-5.85	-6.02	-6.02	-5.77	-6.1	-7.26	-5.94	-5.77	-6.31	-5.74	-5.64	-6.41	-5.68
1YH2	-3.18	-4.52	-7.75	-7.78	-4.19	-5.28	-5.95	-5.67	-5.36	-5.76	-6.2	-6.03	-6.17	-5.1	-5.09	-5.12	-4.92	-5.35	-5.74	-5
1ZDN	-4.09	-5.38	-8.21	-8.69	-4.51	-5.99	-6.29	-5.85	-6.02	-6.02	-5.77	-6.1	-7.26	-5.94	-5.77	-6.31	-5.74	-5.64	-6.41	-5.68
1ZUO	-4.25	-6.12	-11.2	-10.4	-4.51	-6.71	-7.6	-7.19	-6.98	-7.94	-7.74	-7.53	-7.94	-6.49	-7.06	-7.3	-7.1	-6.99	-7.63	-6.97
2A4D	-4.13	-5.09	-8.57	-8.31	-5.25	-5.01	-5.6	-5.19	-6.05	-5.63	-5.7	-5.53	-6.11	-4.91	-4.96	-5.03	-5.27	-5.22	-5.85	-4.86
2A7L	-4.13	-5.15	-9.95	-9.81	-4.23	-4.03	-5.54	-5.96	-5.88	-5.87	-5.39	-5.85	-5.15	-5.3	-5.42	-5.48	-5.7	-5.3	-5.92	-5.29
2AXI	-3.79	-6.3	-7.05	-6.92	-4.57	-7.09	-4.88	-6.64	-7.44	-5.74	-5.32	-5.5	-6.12	-6.96	-5.54	-5.14	-5.6	-7.2	-5.34	-4.8
2ESK	-3.85	-5.45	-8.1	-8.51	-4.52	-6.36	-6.53	-6.46	-6.59	-5.89	-5.62	-6.15	-7.02	-6.06	-6.07	-5.83	-5.68	-6.12	-6.18	-6.1
2F4W	-3.81	-5.28	-9.39	-9.51	-4.21	-5.77	-5.9	-6.17	-6.13	-5.88	-6.17	-6.1	-6.92	-5.71	-6.14	-6.3	-5.78	-6.04	-6.43	-5.94
2FAZ	-3.87	-4.34	-7.68	-7.82	-4.31	-5.24	-5.31	-5.42	-5.8	-5.79	-5.04	-5.48	-6.67	-5.06	-5.15	-5.23	-5.3	-5.18	-6.05	-5.22
2FZP	-4.31	-5.19	-8.62	-8.46	-4.46	-5.25	-6.08	-6.8	-6.22	-6.38	-6.62	-6.23	-6.51	-5.77	-5.95	-5.88	-6.51	-5.73	-6.84	-5.61
2I3H	-3.72	-5.81	-8.79	-9.63	-4.07	-5.18	-6.74	-6.16	-6.29	-6.78	-6.9	-6.41	-5.65	-6.06	-6.03	-6.17	-5.96	-5.77	-7.28	-5.73
2JKU	-3.04	-4.42	-8.07	-8.64	-3.67	-4.37	-5.16	-5.11	-5.06	-5.39	-5.9	-5.11	-4.88	-4.95	-5.16	-5.22	-4.97	-5.63	-5.73	-5.52
2NQ3	-3.48	-5.08	-8.35	-9.19	-4.09	-5.23	-6.2	-5.76	-6.13	-5.88	-6.37	-5.97	-6.01	-5.43	-5.5	-5.53	-5.67	-6.01	-6.31	-5.78
2NSQ	-4.04	-4.94	-9.09	-9.08	-4.77	-5.93	-6	-5.97	-6.9	-5.9	-5.46	-5.6	-6.67	-6.46	-6.2	-5.61	-6.87	-6.41	-6.89	-5.73
2NTE	-3.82	-5.71	-8.54	-9.26	-4.62	-5.72	-5.91	-6.32	-6.09	-7.14	-6.12	-6.98	-6.96	-5.51	-5.94	-6.03	-5.86	-5.8	-7.01	-5.74
2OOA	-3.89	-5.92	-11.6	-9.41	-4.25	-5.52	-6.52	-6.53	-6.58	-6.57	-6.81	-6.66	-6.39	-6.34	-6.3	-6.54	-6.28	-6.45	-6.91	-5.76
2PB7	-4.2	-5.66	-8.35	-8.37	-4.83	-5.76	-6.91	-6.62	-6.64	-6.64	-6.1	-6.7	-7.13	-6.08	-6.67	-6.9	-5.63	-6.91	-6.44	-5.97
2PIE	-4.53	-5.45	-7.96	-8.24	-4.74	-5.32	-5.54	-5.99	-5.76	-5.71	-5.93	-6.31	-7.05	-5.38	-5.47	-5.53	-5.73	-5.55	-5.88	-5.62
2POI	-3.25	-4.63	-7.29	-8.06	-3.98	-5.23	-5.32	-5.6	-5.33	-5.6	-5.33	-5.35	-5.91	-5.28	-5.53	-5.61	-5.04	-5.18	-5.78	-4.79
2UVL	-3.9	-5.82	-10.6	-8.32	-4.68	-6.3	-6.29	-6.1	-6.23	-6.36	-6.8	-6.09	-7.35	-5.74	-5.91	-6.04	-6.07	-5.83	-6.83	-5.73

Table 6 (*Continued*).

	L1	L2	L4	L5	L7	L8	L9	L10	L11	L12	L13	L14	L15	L16	L17	L18	L19	L22	L23	L24
2V40	-4.38	-5.42	-8.98	-10.1	-4.7	-5.72	-6.56	-6.51	-6.19	-6.1	-6.49	-6.7	-6.47	-5.95	-6.02	-6.09	-5.75	-5.81	-6.14	-5.67
2XEU	-3.7	-4.68	-7.47	-7.65	-4.07	-5.21	-5.31	-5.64	-5.74	-5.5	-5.29	-5.91	-6.45	-4.88	-5.28	-5.35	-5.28	-5.06	-6.25	-4.95
2XOC	-3.93	-5.21	-8.85	-8.67	-4.78	-6.95	-7.13	-7.11	-6.92	-7.03	-7.39	-6.84	-7.76	-6.6	-6.99	-7.11	-6.22	-6.61	-6.83	-6.31
2XP0	-3.87	-5.48	-8.22	-8.78	-4.91	-6.7	-6.52	-6.99	-6.61	-6.95	-7.15	-6.14	-7.57	-6.39	-6.77	-6.9	-6.04	-6.28	-6.96	-6.07
2Y1N	-4.78	-6.19	-9.38	-9.2	-5.57	-6.36	-7.19	-6.96	-6.83	-6.44	-6.13	-6.63	-7.31	-6.59	-6.5	-5.92	-6.01	-6.47	-6.26	-6.61
2YVQ	-3.66	-5.08	-8.93	-9.43	-4.77	-5.76	-5.76	-6.44	-6.2	-5.93	-5.99	-6.27	-7.19	-5.61	-5.89	-5.97	-5.75	-5.76	-6.48	-5.02
2YVR	-3.85	-6.17	-8.51	-8.49	-5.46	-4.77	-6.47	-6.91	-6.8	-6.82	-6.29	-6.76	-6.54	-6.57	-6.48	-6.53	-7.1	-6.6	-7.06	-6.34
2Z6O	-4.55	-7.32	-10.3	-10.6	-4.97	-6.07	-7.34	-6.57	-6.44	-6.62	-6.66	-6.64	-7.17	-6	-6.31	-6.53	-6.52	-5.97	-7.11	-6.23
3ASL	-3.26	-3.8	-6.79	-7.08	-4.07	-4.37	-5.07	-5.04	-4.97	-4.99	-5.03	-5.17	-5.55	-4.72	-5.03	-5.21	-4.68	-5.1	-5.52	-4.8
3B08	-3.61	-5.11	-8.36	-8.37	-4.47	-5.28	-5.96	-5.95	-6.11	-6.02	-5.44	-5.65	-6.48	-5.27	-5.37	-5.43	-5.6	-5.39	-6.47	-5.03
3B76	-4.16	-5.72	-10.6	-10.1	-4.46	-5.29	-6.84	-6.52	-6.54	-6.62	-6.65	-6.45	-6.16	-6.13	-6.36	-6.44	-6.41	-6.25	-7.85	-6.38
3B7Y	-3.93	-5.19	-9.26	-9.67	-4.24	-6.29	-5.89	-5.87	-5.97	-6.49	-6.23	-6.14	-7.34	-5.65	-5.94	-5.9	-5.63	-6.11	-6.24	-5.99
3BI7	-3.88	-5.32	-8.41	-8.59	-4.89	-5.53	-6.48	-6.27	-6.33	-6.58	-6.63	-6.5	-6.69	-6.02	-6.4	-6.55	-6.01	-6.06	-6.41	-5.97
3BUX	-4.32	-5	-7.56	-8.37	-4.22	-6.19	-5.72	-5.56	-5.68	-5.66	-5.85	-5.7	-7.23	-5.61	-5.77	-5.83	-5.15	-5.36	-5.71	-5.37
3BZH	-4.21	-6.05	-7.89	-8.54	-4.63	-6.81	-7.08	-7.06	-6.73	-6.96	-7.06	-6.37	-7.42	-6.72	-6.99	-7.08	-6.47	-7.1	-6.76	-6.75
3C5E	-4.34	-5.77	-10.7	-9.9	-4.92	-5.83	-6.72	-6.7	-6.47	-6.84	-6.57	-7.23	-7.74	-5.9	-6.37	-6.49	-6.21	-6.78	-6.78	-6.83

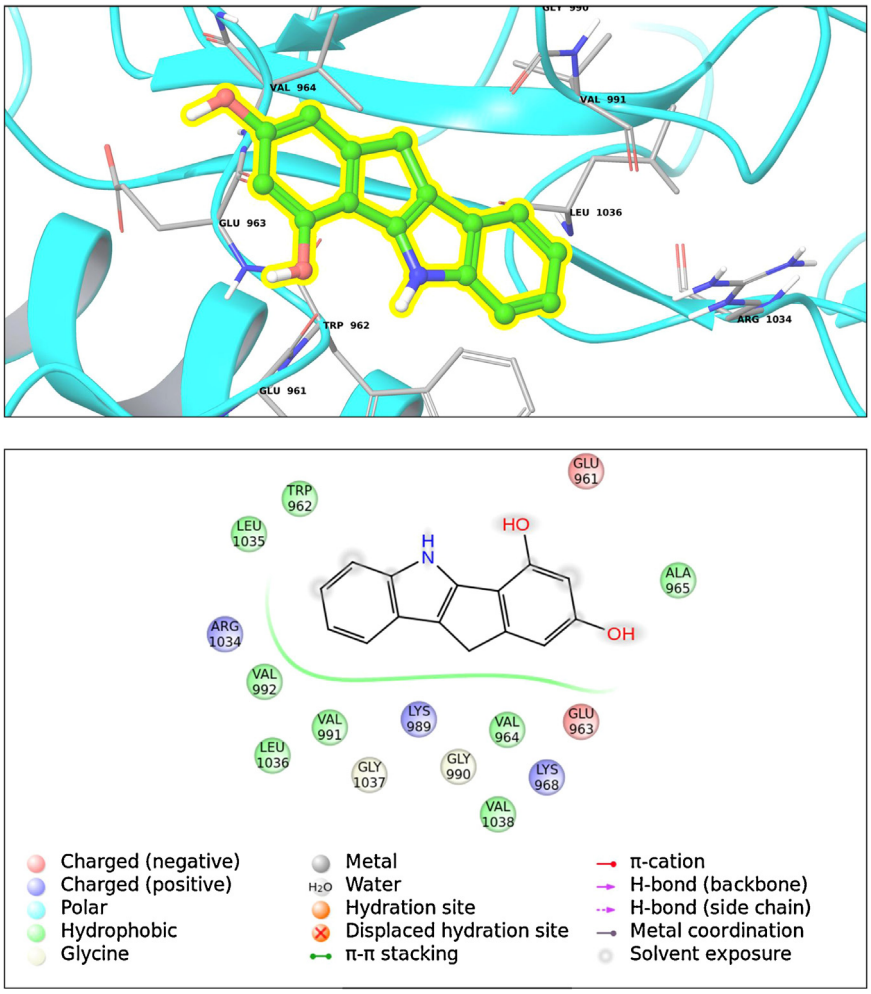

Fig. 1. (Top) Binding interactions for top-docking poses of compound **26** within transferases family (Class II; 1P4O, PDB ID). (Bottom) 2D ligand interaction diagram.

2.1. Preparation of ligand structures

Compounds were prepared with the Schrodinger's Maestro module and then geometry optimization studies were performed for these ligands using Polak-Ribiere conjugate gradient (PRCG) minimization (0.0001 kJ $Å^{-1}$ mol^{-1}, convergence criteria) using Macromodel. Protonation states of ligands and residues were tested using LigPrep and Protein Preparation modules under Maestro molecular modeling package (v.9.2) at neutral pH [15].

2.2. Preparation of protein structures

From Protein Data Bank (PDB) [16] available solved X-ray structures that have less than 2.0 Å resolution is considered (7443 proteins). From these proteins, enzymes with 6 classes are selected (hydrolases, transferases, oxidoreductases, lyases, isomerases, and ligases). To get rid of the statistical bias that may occur because of the homology between proteins, similar sequences at ≥90% identities were removed. From these families, proteins of oxidoreductase (class-I) did not have successful docking poses, so these targets are not considered in further tests. Finally 229 proteins X-ray crystal structures from the PDB [16] were selected and downloaded. After selecting and downloading the protein structures from the database, several procedures were applied in order to make these structures ready for docking. Within these procedures firstly water molecules were removed. Bond orders were assigned and hydrogen atoms necessary for docking were added. Then, restrained minimization of hydrogen atoms was performed. Subsequently, optimization of hydrogen bonds was applied. The coordinate files of proteins are converted into *pqr* format from *pdb via* PDB2PQR server. As a forcefield PARSE options selected to ensure that new atoms are not rebuilt too close to existing atoms, and then, the hydrogen-bonding network were optimized. Finally, to assign protonation states at pH 7, PROPKA was used [17].

2.3. Grid-box generation

The grid parameter file of each protein was generated using AutoDockTool software. During the parameter file preparation process, a grid-box was generated that was large enough to cover the entire protein binding site and accommodate all ligands to move freely. The size of grid box in *x*, *y*, and *z* directions were taken as 126 Å × 126 Å × 126 Å. As grid-space 0.375 Å is considered. The center of mass of the receptor in the X-ray crystal structure was selected as the center of the grid-box. Finally blind docking was performed that covers the whole protein as binding pocket.

2.4. Ligand docking

AutoDock4 and a Lamarckian genetic algorithm (LGA) [18] were used for protein-fixed ligand-flexible docking calculations. Twenty search attempts (*i.e.*, ga_run parameter) were performed for each ligand. The maximum number of energy evaluations before the termination of LGA run was 2,500,000 and the maximum number of

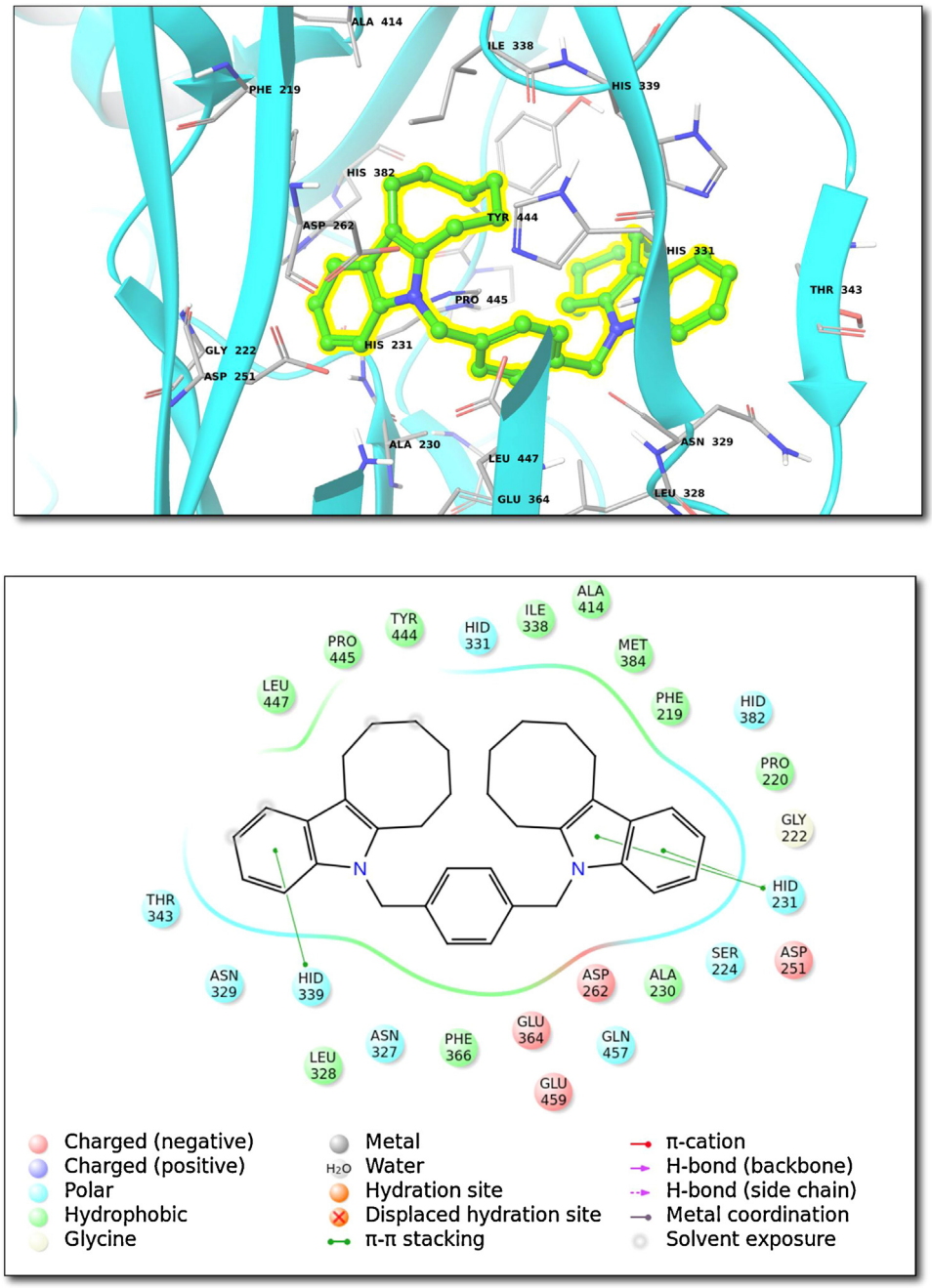

Fig. 2. (Top) Binding interactions for top-docking poses of compound **5** within hydrolases family (Class III; 1B6A (PDB ID)). (Bottom) 2D ligand interaction diagram.

generations of the LGA run before termination was 27,000. Other docking parameters were set to the default values of the software. After docking simulations, the ligands were ranked according to their predicted protein–ligand binding affinity. Finally from the output files of docking analysis, different file conversions were applied for further analysis. Promising ligands are further tested at hERG1 pore domain using Glide/XP Induced Fit Docking (IFD) algorithm [19]. The IFD default protocol was used, consisting of: (i) constrained minimization of the receptor with an RMSD cut-off of 0.18 Å; (ii) initial glide docking (SP) of each ligand using a soft potentials (0.5 van der Waals radii scaling of non-polar atoms of ligands and receptor using partial charge cutoff of 0.15); (iii) derived docking poses were then refined using the Prime module of Schrodinger's molecular modeling package Maestro [15]. Residues within the 5.0 Å of ligand poses were then minimized in order to form suitable conformations of poses at the active site of the receptor. (iv) Glide XP re-docking of each protein–ligand complex were applied.

3. Results and discussion

Multi-targeted hits on certain group of proteins were screened using docking simulations. In particular, 26 ligands were docked at 229 different target receptors. Five classes of proteins were considered for docking [8–10]. More specifically 38 proteins from the lyases, 47 proteins from hydrolases, 47 proteins from transferases, 45 proteins from ligases, and 52 proteins from isomerases were used. Homology similarities between targets used and carbonic anhydrase enyzmes I and II have been given at the Supplementary Figure, Fig. S1. In this study, Autodock Docking Software was used

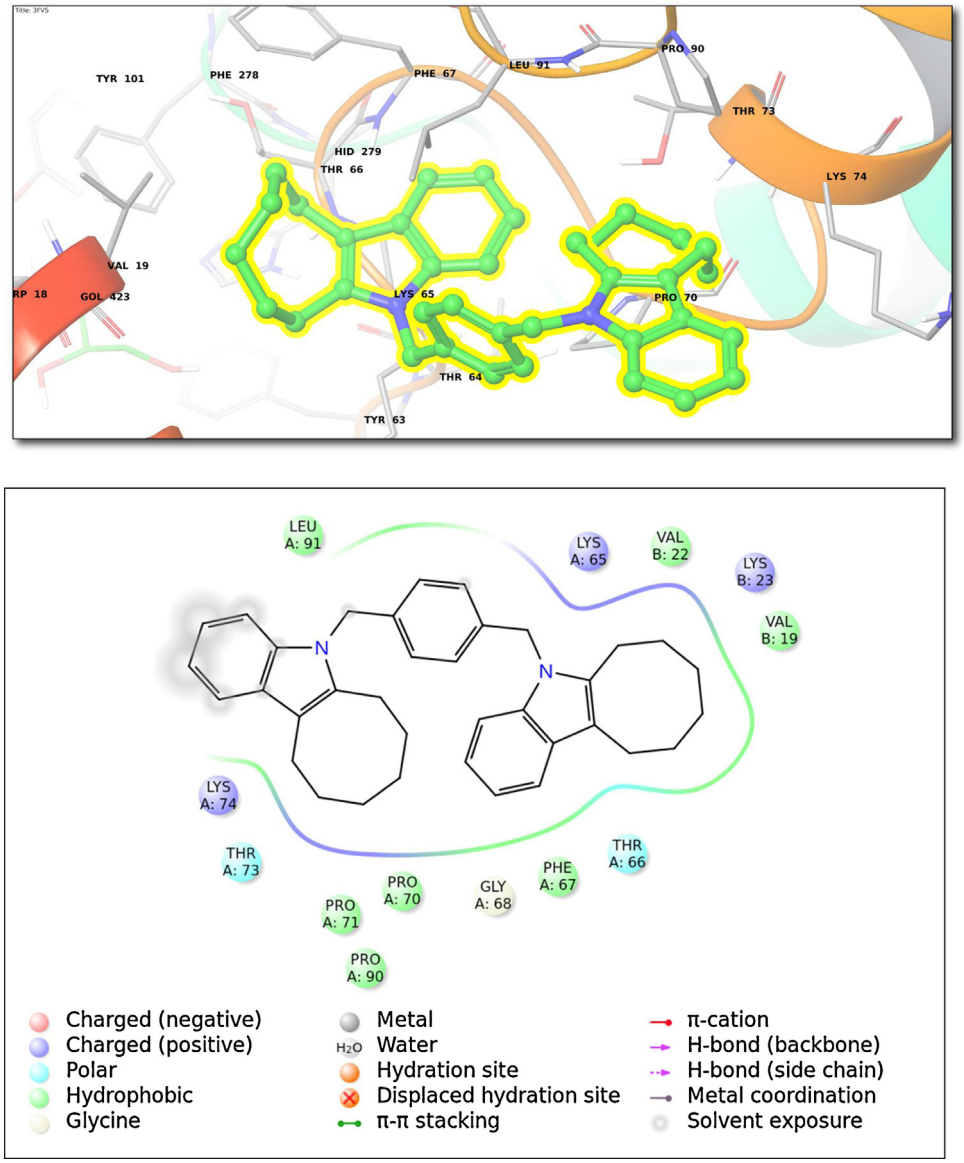

Fig. 3. (Top) Binding interactions for top-docking poses of compound **5** within Lyases family (Class IV; 3FVS (PDB ID)). (Bottom) 2D ligand interaction diagram.

for the computation of the determination of the optimum binding sites and energies. The results on the calculated binding energy values for all proteins in each class were tabulated. Estimated binding energy values of each ligand–protein pair are collected in Tables 2–6. A color-coding was used for a better visualization. We set color map according to a certain threshold values of docking scores. This coloring was applied in order to visualize the grouping of the ligands with different binding affinities. Especially, the hits shown by red color are important since they refer to the best docking scores and high-affinity binding. Accordingly, Tables 2–6 represent docking scores of successful runs of these ligands in Table 1 at different classes of enzymes. Some compounds in Table 1 did not show a successful docking because they could not fit well at the binding pockets of the used targets, thus for these compound docking scores are not recorded.

Considering the docking results that are tabulated at Tables 2–6, compounds **3** and **5** have the top-docking scores for lyases (Class IV), compounds **4** and **5** have the top-docking scores in all three enzymes, namely hydrolases (Class II), isomerases (Class V) and ligases (Class VI); and compounds **3**, **4** and **26** have the lowest binding energy in transferases (Class II). Top-docking poses of transfreases (Class II) are observed for compound **26** and a receptor PDB ID (1P4O). The interaction analysis suggests that the following amino acid residues form binding pocket for compound **26**: Lys968, Glu961, Leu1036, Arg1034, Gly990, Val991, Trp962, Glu963, Val964 and Ala965 (Fig. 1). The cellular functions of 1P4O (insulin-like growth factor 1) receptor involve ATP binding, insulin binding, insulin receptor binding, insulin-like growth factor binding and insulin-like growth factor-activated receptor activity [20]. The high affinity binding found in docking for compound **26** suggests that this CA-inhibitor may be also involved as potential inhibitor targeting this transferase.

Next class enzymes analysed was hydrolases. Compound **5** was found to bind with high-affinity to the following receptor (PDB ID, 1B6A, Hydrolases Class III). The binding pocket organization is shown in Fig. 2. Close contact residues were found as Met384, Ala414, Phe219, Ile338, His339, His331, Glu364, Asn329, Leu328, Asn327, His382, Pro443, Tyr444, His231, Pro445, Asp376, Leu447 (Fig. 2). The 1B6A (human methionine aminopeptidase 2) receptor participates in translation, ribosomal structure and biogenesis. The biochemical function of 1B6A involves metal ion binding, metalloexopeptidase and aminopeptidase activity [21].

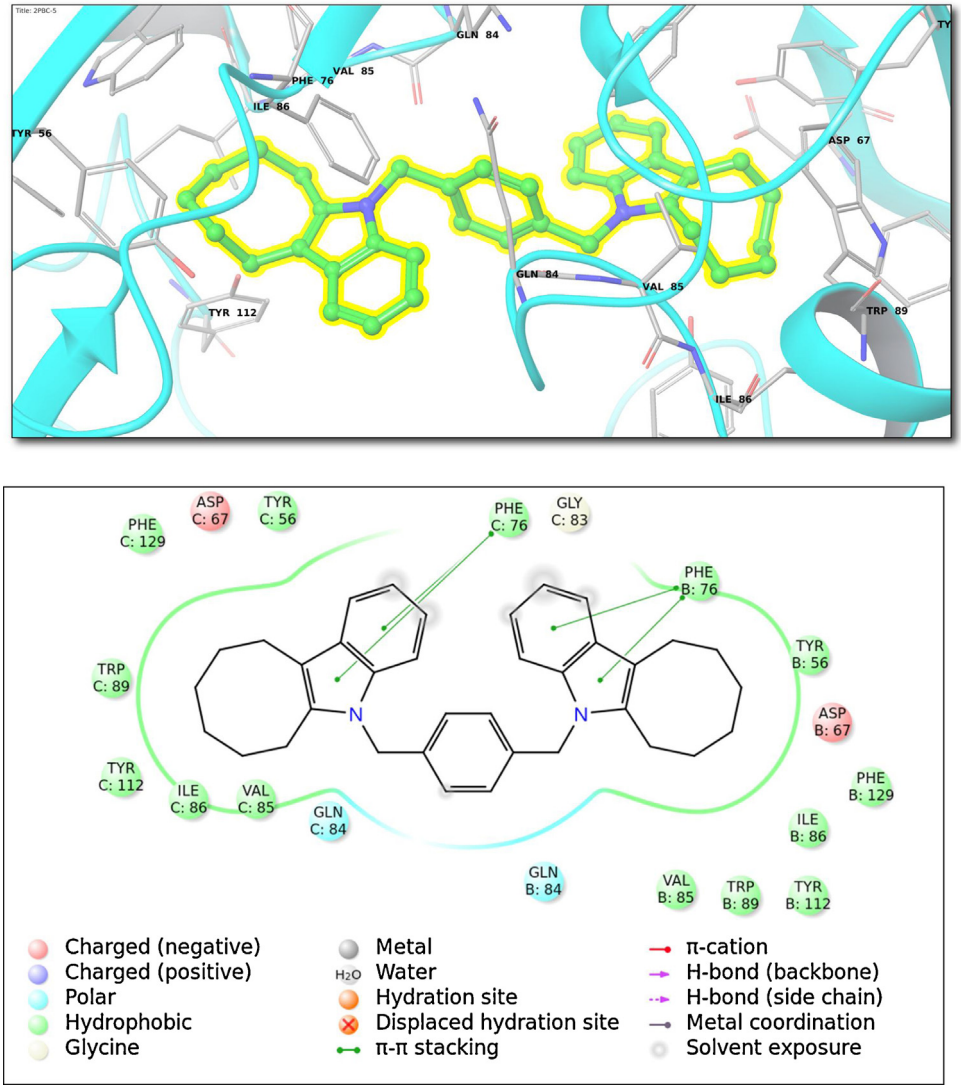

Fig. 4. (Top) Binding interactions for top-docking poses of compound **5** within isomerases family (Class V; 2PBC (PDB ID)). (Bottom) 2D ligand interaction diagram.

Considering the functions of this enzyme, 1B6A, the high-affinity compound **5** as CA-inhibitor, may also have an application in treatments of protein-synthesis related illnesses. The top-docking poses for the compound **5** as the representative from Class-IV lyases (PDB ID, 3FVS) are collected in Fig. 3. The bound ligand (compound **5**) forms close contacts with following amino acid residues: Lys74, Pro90, Pro70, Thr73, Leu91, Lys65, Gly68, Phe67, Thr66, Val22, Val19, and Lys23 (Fig. 3). The human kynurenine aminotransferase I (hKAT I, PDB ID, 3FVS) catalyzes the formation of kynurenic acid, a neuroactive compound. The general functions assigned to 3FVS include amino acid transport, which is essential for many metabolic pathways. Molecular functions of this enzyme are L-glutamine/pyruvate aminotransferase activity, L-phenylalanine-oxaloacetate transaminase activity, L-phenylalanine/pyruvate aminotransferase activity, cysteine-S-conjugate/beta-lyase activity, glutamine/phenylpyruvate transaminase activity, kynurenine/oxoglutarate transaminase activity and pyridoxal phosphate binding [22]. This enzyme previously had been studied for the inhibition studies of human kynurenine aminotransferase Ile/Gln transaminase K by Qian Han et al. [23]. In that study, active sites residues were found as Gly36, Arg398, Tyr101, Asn185, Tyr216, Trp18, and Tyr63 [22]. The top-docking scores at isomerases (Class V) for the compound **5** with (PDB ID, 2PBC). The following amino acids are forming a binding pocket for the drug: Tyr112, Phe129, Tyr56, Phe76, Ile86, Trp89, Val85, Gln84, Gln84, Val85, Ile86, Tyr112, Trp89, Phe76, Tyr56, Asp67, Phe129 (Fig. 4). This enzyme also known as human FK506-binding protein 2 accelerates the folding of proteins. It catalyzes the *cis-trans* isomerization of prolinimidic peptide bonds inoligopeptides [24]. Top-docking poses of target ligases (Class VI) is observed with compound **4** for enzyme with PDB ID, 2OOA. Fig. 5 shows interactions of compound **4** at the 2OOA. Active site is formed by following amino acids: Leu939, Tyr944, Val949, Ala945, Phe946, Glu947, Gly941, Ile936, Ala937, Gly941, Gly943, Glu942, Ala945, Ala937, Tyr944, Phe946, Leu939, Ile936, Asp933, Val949, Lys950 (Fig. 5). 2OOA is an E3 ubiquitin-protein ligase or ubiquitin ligase which combines with specific E2 ubiquitin-conjugating enzymes. E3 ubiquitin-protein ligase which accepts ubiquitin from specific E2 ubiquitin-conjugating enzymes, and transfer it to substrates, generally promoting their degradation by the proteasome [25].

For all the proteins included in this study, overall 4974 different binding energies and binding poses were obtained out of the molecular docking results (metrics for free energy of binding). The free energies of binding obtained from the docking analyses were tabulated for all of these 4974 protein–ligand pairs. Ligands considered in this work had been studied before using GOLD docking program targeting hCA-I and hCA-II isoenzymes [6,7]. The GOLD ChemmScore of compound **5** for binding to

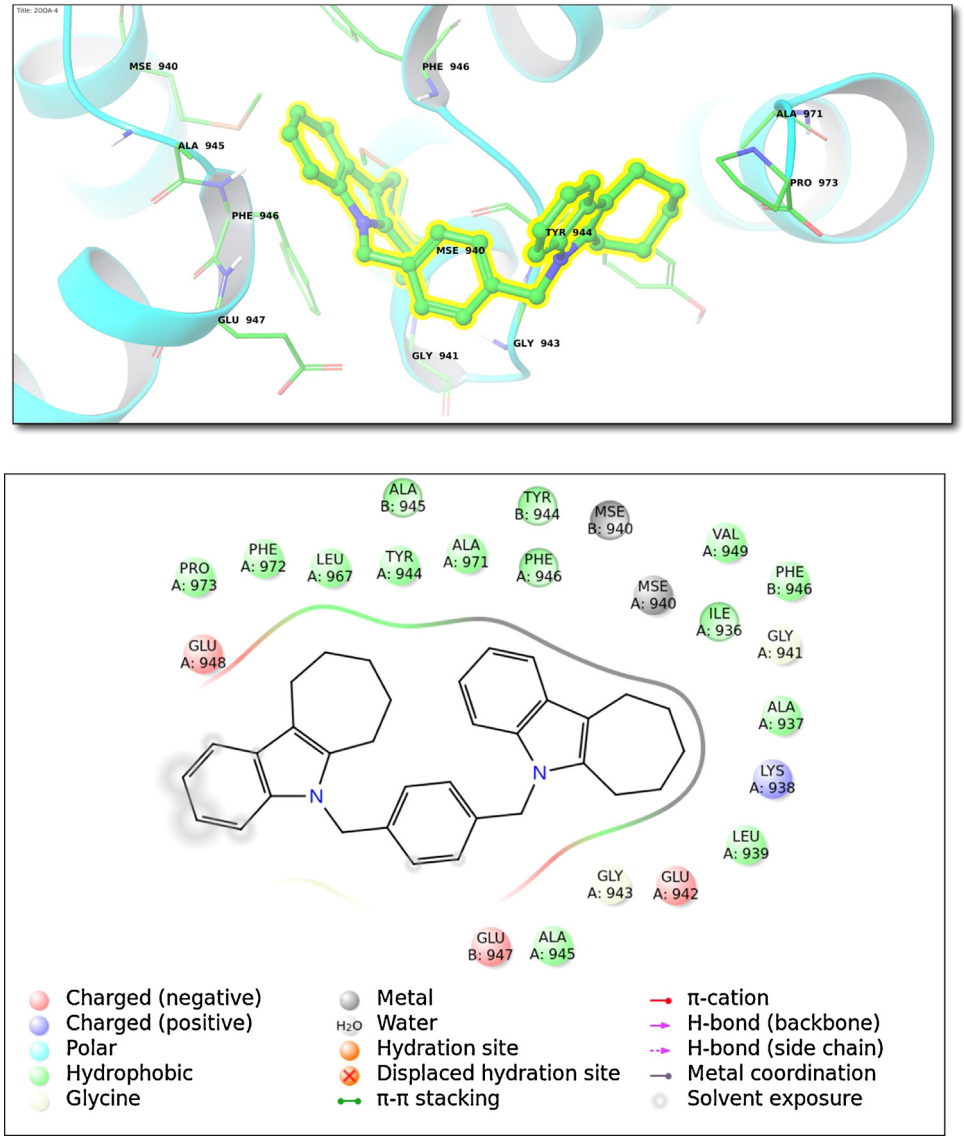

Fig. 5. (Top) Binding interactions for top-docking poses of compound **4** within ligases family (Class VI; 2OOA (PDB ID)). (Bottom) 2D ligand interaction diagram.

hCA-I was −7.88 kcal/mole and a binding pocket was formed by Ala121, Leu131, Ala135, Leu198, Trp5, Pro201, His200, Thr199, His94. In this study, Autodock score of compound **5** with hCA-I is −9.13 kcal/mole and corresponding binding site covers following residues: Ala121, Leu131, Ala135, Leu198, Trp5, Pro201, His200, Thr199, His94, Ala132, Phe91, Asp72, Val143, Leu141. The result from simulations with AutoDock mapped a similar binding site but slightly more favorable binding energy scores. Deriving slightly different docking scores using two different docking programs is expected because of their different scoring algorithms.

The GOLD ChemmScore of compound **5** for binding to hCA-II was −11.61 kcal/mole and binding sites were formed with Phe70, Ile91, Glu69, His119, Val135, Trp123, Gln92, Leu141, Val135, Val121, His122, Leu198, Pro202, and Trp123 [6,7]. In this study, Autodock score of the compound **5** binding to hCA-II is found as −9.29 kcal/mole and binding sites are Pro247, Trp245, Asp243, Val242, Glu14, Pro13, Gly12, Tyr7, Gly16, Lys9, Gly8, Asn11, His10, Phe231, and Glu239. The AutoDock results show different (from GOLD) binding pockets, thus different docking scores compared to reported studies using GOLD force fields. GOLD ChemmScore of compound **3** with hCA-I was −8.01 kcal/mole and binding sites were His94, Phe91, Leu141, Pro201, and His64 [6,7]. The AutoDock score of this compound at the hCA-I is found as −6.62 kcal/mole and binding site residues are Trp209, Thr199, Val143, His119, Leu198, His200, Ala121, His94, Pro202, Gln92, His67, Val62, Phe91, Leu131, Asn69, and Ile60. The AutoDock mapped the same binding site and a similar binding energy score with 1.4 kcal/mole difference. GOLD ChemmScore of compound **3** at hCA-II target was −11.62 kcal/mole and binding sites were Gln92, Phe131, Ile91, Trp123, Val121, Val135, Pro202, Ile91, Glu69, Phe70, Leu141, Leu57 [6,7]. The AutoDock score of this drug at the hCA-II is found as −7.37 kcal/mole and binding site of the compound formed interactions with following residues: Gln92, His119, Val121, Val143, Trp209, Val207, Phe131, Val135, Leu198, Thr199, His94, His96, Thr200, His64, Pro201, Pro202, and Trp5. The results which derived by AutoDock have shown similar binding sites for the drug but binding scores of the compound are underestimated by 4.25 kcal/mole with AutoDock docking algorithm. The variations between the binding energy scores obtained from two different docking softwares, GOLD and AutoDock, might most probably be resulted from the differences in the force field parameters or from the differences in their scoring algorithms [26–28]. However, it must be noted that in most cases both programs led to mapping of similar binding pockets.

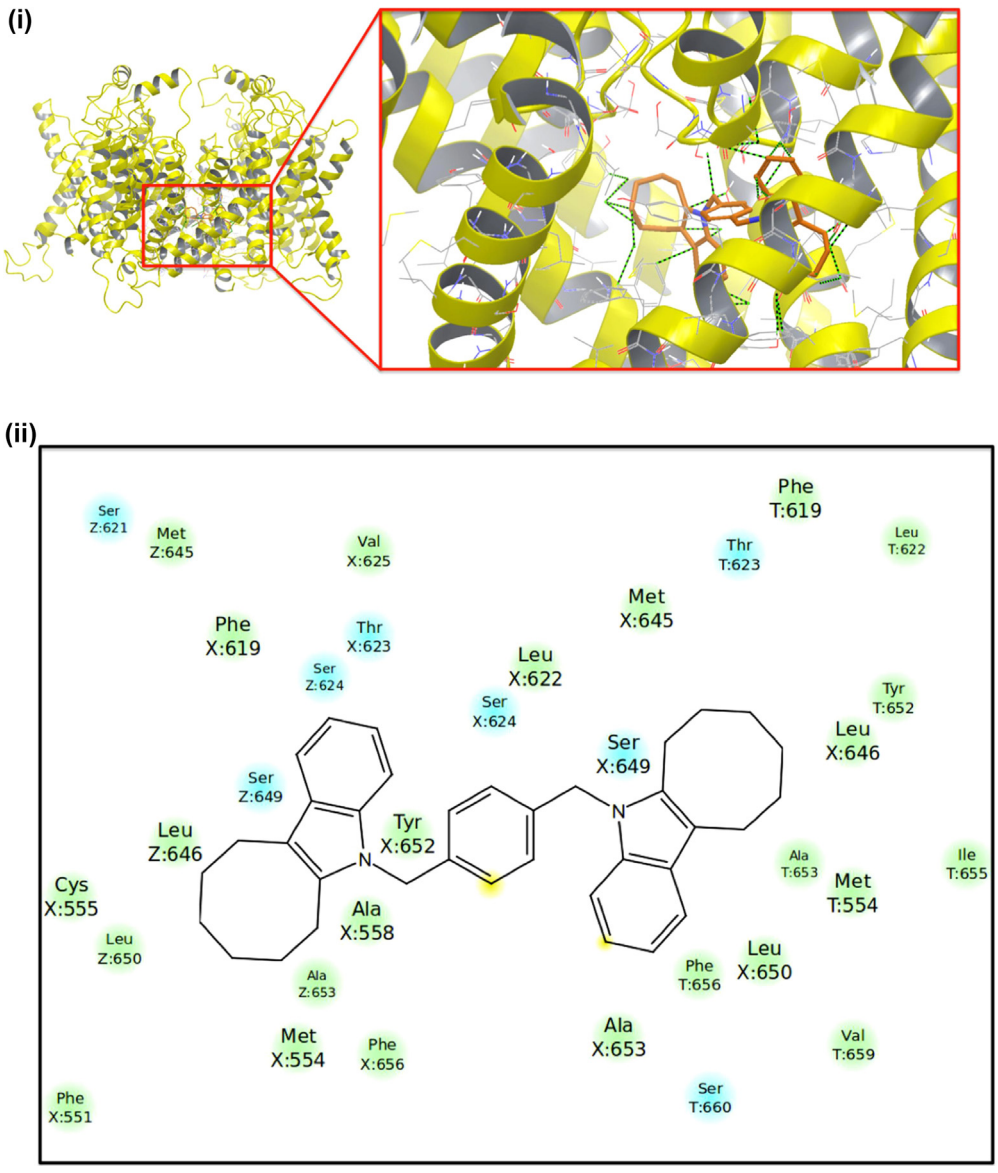

Fig. 6. (i) Top-docking pose of compound **5** at the hERG1 pore domains using Glide/XP Induced Fit Docking. (ii) Corresponding ligand interaction diagram.

In the current study, it is showed that a few compounds (*i.e.*, **3**, **4**, **5**, and **26**) may target several enzymes in addition to their main CA targets (Supplementary Material, Fig. S2). While promising, a cross-target activity is often plagued by unwanted cytotoxic drug interactions with a number of membrane proteins. Several classes of K channels are involved in regulating the heart rate by setting the amplitude and duration of the action potential and the resting membrane potential. Abnormalities in function of these ion channels due to inherited mutations or pharmacological blockage can prolong the duration of the action potential, leading to development of severe arrhythmias (*i.e.*, Long QT syndromes -LQTS). Genetic analysis has revealed that mutations in K channels such as hERG and KvLQT1 form the molecular basis of LQTS [29–34]. The hERG channels are prime target for the pharmacological management of arrhythmias. They are selectively blocked by Class III anti-arrhythmic drugs such as dofetilide and E-4031. K channels are critical to neurotransmission in the nervous system. Alterations of the functions of these channels may lead to severe perturbations in membrane excitability and neuronal function, causing such diseases as episodic ataxia, myokymia and neurodegeneration. Episodic ataxia is linked to mutations in the Kv1.1 potassium channels, benign neonatal epilepsy to KvLQT2 and KvLQT3 channels, and neurodegeneration in Parkinson's disease to Kir3.2 channels. Renal diseases include Bartter's syndrome which is caused by defects in transepithelial transport due to dysfunction of Kir1.1 channels. Such diseases of the heart, central nervous system, and kidneys arise from mutations in K channel genes and/or altered regulations of their function, and may be treated by drugs that modulate their behavior by binding to the active sites on channels. Another dimension of hERG channel is their rather infamous involvement with cardiotoxicity of many drug-like compounds. A broad panel of drug-like molecules from anti-convulstant, anti-histamine, anti-psychotic and anti-depressant families of therapeutic compounds were black-boxed for their ability to block hERG channels.

Thus, compounds **3**, **4**, **5**, and **26** with promising cross-target potential were docked to the pore domain of our previously reported hERG S1-S6 models [8,9]. Results showed that top-docking poses of these compounds have following Induced Fit Docking Glide/XP docking scores: Compound **3** (−9.35 kcal/mole), compound **4** (−10.14 kcal/mole), compound **5** (−10.08 kcal/mole), and compound **26** (−7.92 kcal/mole). Fig. 6 shows binding

interactions of compound **5** and its ligand interaction diagram at the hERG1 pore domain model. Thus, compound **26** has moderate predicted intra-cavitary blocking ability of hERG pore domains, but compounds **3–5** may be involved with a formation of cardiotoxicity and further optimization and refinement studies may be necessary before considering them as multi-targeted agents.

4. Conclusions

Considering our docking results, a few ligands are computed to have highly better binding energies within all classes. Because of the electrostatic properties of the atoms and fulfillment of the proper free volume requirement for the binding process, ligands **4**, **5**, and **26** have the best binding affinities generally. By looking at the dominant red colored columns in Tables 2–6, a number of ligands have high docking scores with many proteins at the same time. According to these simultaneous low binding energies of these ligands, such as compounds **3**, **4**, **5**, and **26** with high number of proteins, we may conclude that such ligands may have multi-targeted effects on different metabolic and illness mechanisms. Multi-functional ligands in different targets have been well addressed in several recent reports [35]. These molecules are then evaluated in hERG protein models that may predict risk and benefits of candidate drugs and may allow molecular "tailoring" for optimal drug design.

Acknowledgements

S.D.'s works are supported by TUBITAK's Co-Funded Brain Circulation program (2236, Project Number: 112C017). S.Y.N. was supported by operating funds from the Canadian Institutes of Health Research (MOP-186232) and Heart and Stroke Foundation of Alberta and NWT Grant-In-Aid funding. S.Y.N. is an Alberta Heritage Foundation for Medical Research Scholar and CIHR New Investigator.

Appendix A. Supplementary data

Supplementary data associated with this article can be found, in the online version, at http://dx.doi.org/10.1016/j.jmgm.2014.02.007.

References

[1] J.J. Lu, W. Pan, Y.J. Hu, Y.T. Wang, Multi-target drugs: the trend of drug research and development, PLoS ONE 7 (2012) e40262.
[2] J.J. Hornberg, Simple drugs do not cure complex diseases: the need for multi-targeted drugs, in: J.R. Morphy, C.J. Harris (Eds.), Designing Multi-Targeted Drugs: RSC, 2012, pp. 1–13.
[3] H. Akazawa, C. Yabumoto, M. Yano, Y. Kudo-Sakamoto, I. Komuro, ARB and cardioprotection, Cardiovasc. Drugs Ther. 27 (2013) 155–160.
[4] A. Bergmann, Method for the identification of patients in need of therapy having minor cognitive disorders and the treatment of such patients. USA, 2011.
[5] A. Fournier, R. Oprisiu-Fournier, J.M. Serot, O. Godefroy, J.M. Achard, S. Faure, H. Mazouz, M. Temmar, A. Albu, R. Bordet, O. Hanon, F. Gueyffier, J. Wang, S. Black, N. Sato, Prevention of dementia by antihypertensive drugs: how AT1-receptor-blockers and dihydropyridines better prevent dementia in hypertensive patients than thiazides and ACE-inhibitors, Expert Rev. Neurother. 9 (2009) 1413–1431.
[6] D. Ekinci, H. Cavdar, S. Durdagi, O. Talaz, M. Senturk, et al., Structure–activity relationships for the interaction of 5,10-dihydroindeno[1,2-b]indole derivatives with human and bovine carbonic anhydrase isoforms I II, III, IV and VI, Eur. J. Med. Chem. 49 (2012) 68–73.
[7] S. Durdagi, M. Senturk, D. Ekinci, H.T. Balaydin, S. Goksu, et al., Kinetic and docking studies of phenol-based inhibitors of carbonic anhydrase isoforms I, II IX and XII evidence a new binding mode within the enzyme active site, Bioorg. Med. Chem. 19 (2011) 1381–1389.
[8] G. Moss, Enzyme Nomenclature, University of London, Queen Mary, 2011 http://www.chem.qmul.ac/uk/iubmb/enzyme
[9] R. Horton, L.A. Moran, G. Scrimgeour, M. Perry, D. Rawn, Principles of Biochemistry, 4th ed., Pearson Education, USA, 2005.
[10] W. Becker, L.J. Kleinsmith, J. Hardin, G.P. Bertoni, The World of the Cell, Benjamin Cummings, San Francisco, 2008.
[11] S. Durdagi, S. Deshpande, H.J. Duff, S.Y. Noskov, Modeling of open closed, and open-inactivated states of the hERG1 channel: structural mechanisms of the state-dependent drug binding, J. Chem. Inf. Model. 52 (2012) 2760–2774.
[12] J. Subbotina, V. Yarov-Yarovoy, J. Lees-Miller, S. Durdagi, J.Q. Guo, et al., Structural refinement of the hERG1 pore and voltage-sensing domains with ROSETTA-membrane and molecular dynamics simulations, Protein Struct. Funct. Bioinf. 78 (2010) 2922–2934.
[13] http://autodock.scripps.edu/resources/adt
[14] http://accelrys.com/products/discovery-studio/
[15] Schrodinger, Inc., New York, 2009.
[16] http://www.rcsb.org/pdb/home/home.do
[17] http://nbcr-222.ucsd.edu/pdb2pqr_1.8/
[18] G.M. Morris, D.S. Goodsell, R.S. Halliday, R. Huey, W.E. Hart, R.K. Belew, A.J. Olson, Automated docking using a Lamarckian genetic algorithm and empirical binding free energy function, J. Comput. Chem. 19 (1998) 1639–1662.
[19] W. Sherman, T. Day, M.P. Jacobson, R.A. Friesner, R. Farid, Novel procedure for modeling ligand/receptor induced fit effects, J. Med. Chem. 49 (2006) 534–553.
[20] http://www.uniprot.org/uniprot/P%209%200806
[21] http://www.uniprot.org/uniprot/P%209%205057
[22] http://www.uniprot.org/uniprot/Q%203%201677
[23] Q. Han, H. Robinson, T. Cai, D.A. Tagle, J. Li, J. Med. Chem. 52 (2009) 2786–2793.
[24] http://www.uniprot.org/uniprot/P%205%202688
[25] http://www.uniprot.org/uniprot/Q%201319%201
[26] A. Politi, S. Durdagi, P. Moutevelis-Minakakis, G. Kokotos, T. Mavromoustakos, Development of accurate binding affinity predictions of novel renin inhibitors through molecular docking studies, J. Mol. Graph. Model. 29 (2010) 425–435.
[27] S. Durdagi, M.G. Papadopoulos, P.G. Zoumpoulakis, C. Koukoulitsa, T. Mavromoustakos, A computational study on cannabinoid receptors and potent bioactive cannabinoid ligands: homology modeling, docking, de novo drug design and molecular dynamics analysis, Mol. Divers. 14 (2010) 257–276.
[28] T. Mavromoustakos, S. Durdagi, C. Koukoulitsa, M. Simcic, M.G. Papadopoulos, M. Hodoscek, S.G. Grdadolnik, Strategies in the rational drug design, Curr. Med. Chem. 18 (2011) 2517–2530.
[29] S. Durdagi, J.Q. Guo, J.P. Lees-Miller, S.Y. Noskov, H.J. Duff, Structure-guided topographic mapping and mutagenesis to elucidate binding sites for the human ether-a-go-go-related gene 1 potassium channel (KCNH2) activator NS1643, J. Pharmacol. Exp. Ther. 342 (2012) 441–452.
[30] S. Durdagi, H.J. Duff, S.Y. Noskov, Combined receptor and ligand-based approach to the universal pharmacophore model development for studies of drug blockade to the hERG1 pore domain, J. Chem. Inf. Model. 51 (2011) 463–474.
[31] S. Durdagi, J. Subbotina, J. Lees-Miller, J. Guo, H.J. Duff, et al., Insights into the molecular mechanism of hERG1 channel activation and blockade by drugs, Curr. Med. Chem. 17 (2010) 3514–3532.
[32] S. Durdagi, C. Zhao, J.E. Cuervo, NoskovF S.Y., Atomistic models for free energy evaluation of drug binding to membrane proteins, Curr. Med. Chem. 18 (2011) 2601–2611.
[33] S. Durdagi, S. Yu. Noskov, Mechanism of K+/Na+ selectivity in potassium channels from the perspective of the nonselective bacterial channel NaK, Channels 5 (2011) 198–200.
[34] Shagufta, D. Guo, E. Klaasse, H. de Vries, J. Brussee, L. Nalos, M.B. Rook, M.A. Vos, M.A.G. van der Heyden, A.P. Ijzerman, Exploring chemical substructures essential for hERG K+ channel blockade by synthesis and biological evaluation of dofetilide analogues, ChemMedChem 4 (2009) 1722–1732.
[35] T. Tzoupis, G. Leonis, G. Megariotis, C.T. Supuran, T. Mavromoustakos, M.G. Papadopoulos, Dual inhibitors for aspartic proteases HIV-1 PR and Renin: advancements in AIDS–hypertension–diabetes linkage via molecular dynamics, inhibition assays, and binding free energy calculations, J. Med. Chem. 55 (2012) 5784–5796.